

NASA TECHNICAL NOTE

NASA TN D-3213

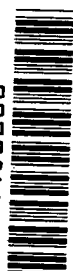


NASA TN D-3213

c. 1

LOAN COPY: 1
AFWL (V)
Kirtland AFB

0079864



TECH LIBRARY KAFB, NM

GROUND EFFECTS ON SINGLE-AND MULTIPLE-JET VTOL MODELS AT TRANSITION SPEEDS OVER STATIONARY AND MOVING GROUND PLANES

by Raymond D. Vogler
Langley Research Center
Langley Station, Hampton, Va.



NATIONAL AERONAUTICS AND SPACE ADMINISTRATION • WASHINGTON, D. C. • JANUARY 1966



0079864

GROUND EFFECTS ON SINGLE- AND MULTIPLE-JET
VTOL MODELS AT TRANSITION SPEEDS OVER
STATIONARY AND MOVING GROUND PLANES

By Raymond D. Vogler

Langley Research Center
Langley Station, Hampton, Va.

NATIONAL AERONAUTICS AND SPACE ADMINISTRATION

For sale by the Clearinghouse for Federal Scientific and Technical Information
Springfield, Virginia 22151 - Price \$3.00

GROUND EFFECTS ON SINGLE- AND MULTIPLE-JET
VTOL MODELS AT TRANSITION SPEEDS OVER
STATIONARY AND MOVING GROUND PLANES

By Raymond D. Vogler
Langley Research Center

SUMMARY

An investigation was made to determine ground effects and jet-free-stream interference effects on the longitudinal characteristics of a VTOL wing-fuselage model at low forward speeds and equipped with various interchangeable arrangements of single and multiple vertical jets. In-ground-effect data were obtained with the model over a stationary ground plane and over a ground plane moving with free-stream velocity.

Out of ground effect all configurations showed interference lift losses and nose-up pitching moments that increased with the ratio of the effective free-stream-to-jet velocity. With the model 1 or 2 effective jet diameters above the ground plane, the data showed large additional losses in lift for some configurations and reduced losses for other configurations when compared with the out-of-ground-effect data. The additional pitching-moment increments also varied with configurations, but the moment changes did not parallel the lift changes. The difference in effects between a ground plane moving with free-stream velocity and a stationary ground plane was small except at the highest velocity ratios with the model 1 effective jet diameter from the ground plane. Under these conditions, the model over the moving ground plane experienced slightly less lift loss and a small nose-up increment in pitch for most configurations.

INTRODUCTION

Considerable research is being done toward the development of vertical take-off and landing (VTOL) airplanes to be used in areas where conventional landing facilities are not available. Jet-supported VTOL models are one of several types that have been investigated (for example, refs. 1 to 4). These investigations have shown that lift losses occur when the model is hovering near the ground and that jet-induced lift losses and nose-up pitching moments occur in transition speeds. These jet-induced lift losses and moment changes result from interference effects between the jet, the free stream, and the model. The interference effects on the aerodynamic characteristics of the model used in the present investigation are reported in reference 4 for transition speeds out of ground effect. Also reported are the characteristics of the

model in ground effect at zero forward speed. The purposes of the present investigation were to determine the combined effects of the ground and forward speed on the losses in lift and nose-up pitching moments and to make a comparison of data obtained with the model over a stationary and a moving ground plane. Heretofore data on VTOL models have been obtained over stationary ground planes, but a ground plane moving with free-stream velocity better represents actual flight conditions (ref. 5). Since the model had no inlets exposed to free stream, any inlet effects on the total force and moment data are not included.

SYMBOLS

The force and moment data are presented about the stability axes and positive directions are indicated in figure 1. The units of measure used in this report are given both in the U.S. Customary Units and, parenthetically, in the International System of Units (SI). (See ref. 6.)

\bar{c}	mean aerodynamic chord, inches (centimeters)
D	drag, including jet force, pounds force (newtons)
d_e	effective diameter, diameter of a circle equivalent in area to total jet-exit area of a given configuration, 3.5 inches (8.89 centimeters)
h	height above ground plane measured from lower surface of fuselage, inches (centimeters)
L	lift, including jet force, pounds force (newtons)
M	pitching moment, including jet moment, inch-pounds force (centimeter-newtons)
q	free-stream dynamic pressure, pounds force/foot ² (newtons/meter ²)
T	resultant measured jet thrust, $\sqrt{L^2 + D^2}$ when $\alpha = 0$ and $q = 0$, pounds force (newtons)
V_j	jet velocity, based on isentropic expansion from jet-exit total pressure to tunnel static pressure, feet/second (meters/second)
V_∞	free-stream velocity, feet/second (meters/second)
α	wing or fuselage angle of attack, degrees
δ_j	jet deflection angle, $\tan^{-1} D/L$ when $\alpha = 0$ and $q = 0$, positive when measured from vertical axis rearward, degrees
ρ_j	mass density in jet exit, slugs/foot ³ (kilograms/meter ³)

ρ_{∞} mass density of free stream, slugs/foot³ (kilograms/meter³)

$\sqrt{\frac{\rho_{\infty} V_{\infty}^2}{\rho_j V_j^2}}$ effective velocity ratio

MODEL AND APPARATUS

A three-view drawing of the model is shown in figure 1 and a photograph is presented as figure 2. The wing, made of 0.125-inch-thick (0.317 cm) aluminum plate with rounded leading and trailing edges, was mounted flush with the top flat surface of the fuselage. The nose of the fuselage was made of wood and the rear section, of sheet metal. The central section of the fuselage was a steel pressure box with a removable bottom which permitted changing the jet configuration. The six different jet configurations, all with equal total exit areas, are shown in figure 3. A detailed drawing of the pressure box and the tubing which supplied air is shown in figure 4. A separate nonpressurized circular chamber in the top of the fuselage enclosed a six-component strain-gage balance on the end of the mounting sting which projected from the floor of the 17-foot test section of the Langley 300-MPH 7- by 10-foot tunnel.

Air entered the model through 0.75-inch-diameter (1.90 cm) tubing which was firmly anchored to the sting near the top of its vertical arm. The air line branched into two lines at the manifold and entered the model on either side of the sting. The lines from the model to the anchor point were shielded from the free stream. The tubing inside the pressure chamber had many small holes which distributed the air in the upper section of the chamber. The chamber was divided by a perforated plate and wire screen to give a more uniform distribution of air in the lower part of the chamber. Jet velocities were determined by a single total-pressure probe inserted at the center of the round jets and at two or three positions in the slotted jets.

The moving ground plane (fig. 4) was obtained by means of a fabric belt between two rollers driven by an electric motor. The ground plane was 144 inches (366 cm) wide by 121 inches (307 cm) long. The boundary layer on the tunnel floor upstream of the belt was removed with a suction slot just upstream of the moving ground plane. Boundary-layer buildup on the moving ground plane could be prevented by making the belt velocity approximately equal to the free-stream velocity. The effect of the moving belt on the boundary-layer profile is shown in figure 5.

TEST CONDITIONS AND ACCURACY

Tests at forward velocity were for an angle-of-attack range from -5° to 20° except when limited by the distance from the model to the ground plane which varied from 1 to 9 effective jet diameters. The tunnel free-stream velocities were 30, 60, and 100 fps (9.14, 18.29, and 30.48 m/s) and when the ground plane

was moving, its velocity was approximately the same as the free-stream velocity. Jet velocities were 400 and 570 fps (121.92 and 173.73 m/s). In addition to the tests made with the model at forward velocity, some tests were made at zero forward velocity at $\alpha = 0^\circ$ through a range of model heights or distances from the ground plane.

The attempt to get uniform velocity through the multiple nozzles by perforating the divider plate and using a wire screen was not entirely successful. The maximum velocity variation among nozzles of a given configuration was as much as 5 percent for the round nozzles, but was less for the ends of the slotted nozzles. Usually, the higher velocity flowed through the upstream nozzles and thus caused the apparent axes of the jets, as determined from static lift and drag forces, to be tilted downstream approximately 1° to 4° ($\delta_j \approx 1^\circ$ to 4°). Both of these conditions are the reverse of conditions that existed when this model was used in a previous investigation (ref. 4). One explanation is that the wire screen which was in the downstream end of the pressure chamber may have corroded since the previous investigation; hence, the size of the screen openings may have been reduced.

The ground-plane belt, still or moving, usually was flat on the supporting plate, but on some occasions wrinkles would appear in the belt as a result of jet impact when the tension in the belt had been reduced by high atmospheric humidity. Usually the wrinkles could be prevented by adjusting the tension in the belt and applying a partial vacuum to the bottom side of the belt through perforations in the supporting plate. The wrinkles, produced by the high velocity jet when the model was close to the belt, were usually about parallel to the fuselage and were near the wing-fuselage juncture. For the configuration with the long central slot, the wrinkles were not completely eliminated. There is some doubt about the reliability of the data for this configuration at effective velocity ratios of 0.25 and 0.17 when the model is as close to the ground plane as 2 effective jet diameters. Wrinkles, if not eliminated, would change the effective height of the model when the model is close to the ground plane. They did not appear when the model was farther away than 2 or 3 effective jet diameters.

The expansion and contraction of the air line between the model and the point where the line is anchored to the sting may be a source of error in the drag data. Moderately large temperature changes occur in the air line and may change the zero setting of the drag gage. Most of this source of error was eliminated by allowing the temperature to stabilize before taking any data, but some error was inevitable.

Although the accuracy of the data is not considered to be as good as that usually obtained without a moving ground board and without air lines attached to the model, it is believed that the ratios L/T , D/T , and $M/T\bar{c}$ are accurate within ± 0.04 , ± 0.02 , and ± 0.02 , respectively. This belief is based on repeatability of data, changes in zero settings of balance gages before and after test runs, and general scatter in the plotted data.

RESULTS AND DISCUSSION

The force and moment data of this investigation have been nondimensionalized by the measured static thrust at zero tunnel speed and out of ground effect. For each configuration two thrust conditions and three tunnel speeds were combined to give a range of effective velocity ratio $\sqrt{\frac{\rho_{\infty} V_{\infty}^2}{\rho_j V_j^2}}$ covering the transition speed range. The effective velocity ratio, suggested in reference 5 and which involves the densities, appears to be a more logical parameter than just the velocity ratio if cold-jet data are to be applicable to hot jets. The six configurations used in this investigation represent some possible single- and multiple-engine combinations in the fuselage.

Zero Angle of Attack

Data for the configurations at zero angle of attack are given in figure 6 for various tunnel speeds and heights of the model over a horizontally moving ground plane. The ground-plane velocity is approximately equal to free-stream velocity. For all configurations there is no loss in lift ($L/T = 1$) in hovering ($V_{\infty} = 0$) if the model is at least 7 effective jet diameters above the ground plane. However, if the model is in forward flight ($V_{\infty} > 0$), there are lift losses which increase with flight velocity or, more properly, with effective velocity ratio. Near the ground plane some configurations show large losses in lift and some large gains, with or without forward velocity. As the jet impinges on the ground plane, it is forced to flow horizontally. This horizontal flow between the fuselage and the ground plane reduces the pressure under the fuselage and wing and produces the loss in lift close to the ground plane as shown for configurations 1 and 2. However, if two or more jets are used, some combinations will produce conditions in which the horizontal flow will be mutually blocked and the result will be an increase in pressure under the fuselage between the jets and a gain in lift, as shown by configuration 3 of figure 6. The loss in lift away from the ground plane at forward speeds results from reduced pressure on the fuselage which is caused by the interference between the free stream, the jet, and the model. As reported in reference 7, the pressure measurements on a flat plate with a jet issuing normal to the plate indicate a small region of increased pressures upstream of the jet and a larger region of markedly reduced pressures downstream of the jet.

The reduced pressures downstream of the jets in forward flight produce the nose-up pitching moments on this model and are typical of the moments of other jet VTOL models (refs. 1 to 4). It will be noted that the more streamlined configurations (configurations 2 and 3) have smaller pitching moments than the other configurations. At zero forward speed near the ground plane, the pitching moments are usually small, although the lift losses or gains may be large. When there is no forward velocity, the horizontal flow is in all directions and the lift increments are distributed symmetrically about the jet center or group center if the group is nearly symmetrical. However, swept wings low on the fuselage increase the nose-up moments while the model is hovering close to the ground. (See ref. 4.)

The variations in drag-thrust ratio with distance above the ground plane (fig. 6) are small and within the accuracy of the data for any given effective velocity ratio. Variations in drag with effective velocity ratio result from a combination of aerodynamic drag and the drag component of the thrust. Comparisons of the magnitude of the drag between configurations would not be valid because the drag includes a small thrust component which is not the same for each configuration.

A comparison of the data obtained with the model over a still and a moving ground plane is shown in figure 7. The effective velocity ratio and model attitude were held constant as the model height from the ground plane was varied. Data points for similar runs at $h/d_e = 9.1$ for the still and the moving ground plane should coincide since the model is essentially out of ground effect. The difference in value between these two points is an indication of the repeatability of the data. It is unlikely that any single nonannular jet would show an increase in lift-thrust ratio near the ground plane such as that shown at $h/d_e = 0.5$ for the two highest effective velocity ratios in figure 7(b). This increase was probably caused by wrinkles in the ground plane giving an upward velocity to the jet after impingement. Multiple jets may show an increase in lift-thrust ratio, the magnitude of the increase depending upon such factors as their geometric arrangement, height from the ground plane, and ratio of the plate area inside the jet group to the area outside. In general, the data of figure 7 show little or no effect of the moving ground plane for the configurations at zero angle of attack. There is some indication of a slight effect, however, when the model is very near the ground plane. Data taken 1 and 2 effective jet diameters from the ground plane for an angle-of-attack range are presented in subsequent figures.

Variable Angle of Attack

Out of ground effect.- The longitudinal characteristics of the various model configurations out of ground effect are presented in figure 8 for an angle-of-attack range for several effective velocity ratios. The interference losses in lift shown earlier (fig. 6) at zero angle of attack are about constant throughout the angle-of-attack range (ref. 4), but the aerodynamic lift of the wing increases with angle of attack and dynamic pressure to give an increasing value of the lift-thrust ratio. The increase in dynamic pressure also produces stronger interference effects under the rearward part of the model which result in an increase in nose-up pitching moments. The negative drag at zero angle of attack for some configurations results from the rearward tilt of the jet axes.

In ground effect.- Data obtained over a still and a moving ground plane are presented in figures 9 and 10 for model heights of 2 and 1 effective jet diameters. These heights are measured at $\alpha = 0^\circ$. As the angle of attack is changed, the model moves upstream or downstream on a circular arc, the center of which is 38 inches (96.52 cm) above the ground plane. Thus, an angle-of-attack change also results in a corrected height of the moment center as represented by the following equation:

$$\left(\frac{h}{d_e}\right)_{\text{Corrected}} = \frac{h}{d_e} + \left(10.85 - \frac{h}{d_e}\right)(1 - \cos \alpha)$$

The maximum correction (at $\alpha = 10^\circ$) would increase the model height in effective jet diameters from 1 and 2 to 1.15 and 2.13. Also, any point of the model ahead or behind the moment center would be higher or lower than the moment center by its distance times $\sin \alpha$. Such variations in height should not invalidate comparison of data for the still and the moving ground plane. Differences in the drag data between those obtained over a still and a moving ground plane are generally within the accuracy of the data, although at the highest dynamic pressures a small reduction in the drag is indicated for some configurations when the ground plane is moving.

The effect of the moving ground plane on the lift and pitching moments is more clearly shown by cross-plotting the data of figures 9 and 10 for given angles of attack and velocity ratios. The cross plots are presented in figures 11 and 12. Also shown in these figures are the out-of-ground-effect data from figure 8 for the same angles of attack and velocity ratios.

The effects on the lift-thrust ratios of the moving ground plane are little different from those of the still ground plane with possible exceptions at high effective velocity ratios (fig. 11). At the highest effective velocity ratio (0.25) and at a model height of 1 effective jet diameter, the moving ground plane gives slightly larger lift-thrust ratios (less lift loss) than the still ground plane. This difference is generally reduced or eliminated at lower effective velocity ratios or at greater distances from the ground plane. Also, any differences between the moving and still ground planes vary little with angle of attack for the range shown.

At the higher effective velocity ratios the increments of moment-thrust ratios between the moving and the still ground planes shown in figure 12 follow the trends of the lift-thrust differences between the two ground planes shown in figure 11. Usually, a lift increment produced by the moving ground plane is accompanied by an increment in nose-up pitching moment.

The most obvious results shown in figure 11 are the large differences in lift-thrust ratio between in and out of ground effect. The reduction in lift out of ground effect with increasing effective velocity ratios at $\alpha = 0^\circ$ results from interference. As the angle of attack is changed, the wing effect is added to the jet effect. For some configurations (configurations 2, 4, and 6) the ground effect is very large and differences between the moving and the still ground plane are almost insignificant when compared with the total ground effect. The large ground effect on the lift generally results in large changes in the magnitude of the pitching moments (fig. 12), but the direction of the pitching-moment increments could not readily be inferred from the lift increments. The ground effect combined with the interference effects resulted in reduced lift and pitching moments for the single-round-jet configuration (configuration 1), reduced lift and increased moments for the central-slotted-jet configuration (configuration 2), increased lift and reduced moments for the four-jet rectangular configuration (configuration 4), and increased lift and moments for most of the other configurations, when compared with the out of ground effect.

CONCLUDING REMARKS

An investigation was made to determine ground effects and jet-free-stream interference effects on the longitudinal characteristics of a wing-fuselage VTOL model moving at low forward speeds and equipped with various interchangeable arrangements of single and multiple jets. In-ground-effect data were obtained with the model over a stationary ground plane and over a ground plane moving with approximately free-stream velocity.

Out of ground effect, all configurations showed interference lift losses and nose-up pitching moments that increased with the ratio of the effective free-stream-to-jet velocity. Configurations with the more streamlined arrangement of the jets had smaller pitching-moment increments. With the model at 1 or 2 effective jet diameters above the stationary ground plane, the data showed large additional losses in lift for some configurations and reduced losses for other configurations when compared with the out-of-ground-effect data. The additional pitching moments also varied with configurations, but the moment changes did not parallel the lift changes. The single-round-jet configuration showed reduced lift and pitching moments; the central-slotted-jet configuration showed reduced lift and increased moments; the four-jet rectangular configuration showed increased lift and reduced moments; and most of the other configurations showed increased lift and moments. The difference in effects between a ground plane moving with free-stream velocity and a stationary ground plane was generally small; however, at the highest effective velocity ratio (0.25) and at a model height of 1 effective jet diameter, the moving ground plane gave slightly larger lift-thrust ratios (less lift loss) and positive pitching moments than did the stationary ground plane.

Langley Research Center,
National Aeronautics and Space Administration,
Langley Station, Hampton, Va., November 4, 1965.

REFERENCES

1. Otis, James H., Jr.: Induced Interference Effects on a Four-Jet VTOL Configuration With Various Wing Planforms in the Transition Speed Range. NASA TN D-1400, 1962.
2. Vogler, Raymond D.; and Kuhn, Richard E.: Longitudinal and Lateral Stability Characteristics of Two Four-Jet VTOL Models in the Transition Speed Range. NASA TM X-1092, 1965.
3. Spreemann, Kenneth P.: Investigation of Interference of a Deflected Jet With Free Stream and Ground on Aerodynamic Characteristics of a Semispan Delta-Wing VTOL Model. NASA TN D-915, 1961.
4. Vogler, Raymond D.: Interference Effects of Single and Multiple Round or Slotted Jets on a VTOL Model in Transition. NASA TN D-2380, 1964.
5. Williams, John; and Butler, Sidney F. J.: Further Developments in Low-Speed Wind-Tunnel Techniques for VSTOL and High-Lift Model Testing. AIAA Aerodynamic Testing Conf., Mar. 1964, pp. 17-32.
6. Mechtly, E. A.: The International System of Units - Physical Constants and Conversion Factors. NASA SP-7012, 1964.
7. Vogler, Raymond D.: Surface Pressure Distributions Induced on a Flat Plate by a Cold Air Jet Issuing Perpendicularly From the Plate and Normal to a Low-Speed Free-Stream Flow. NASA TN D-1629, 1963.

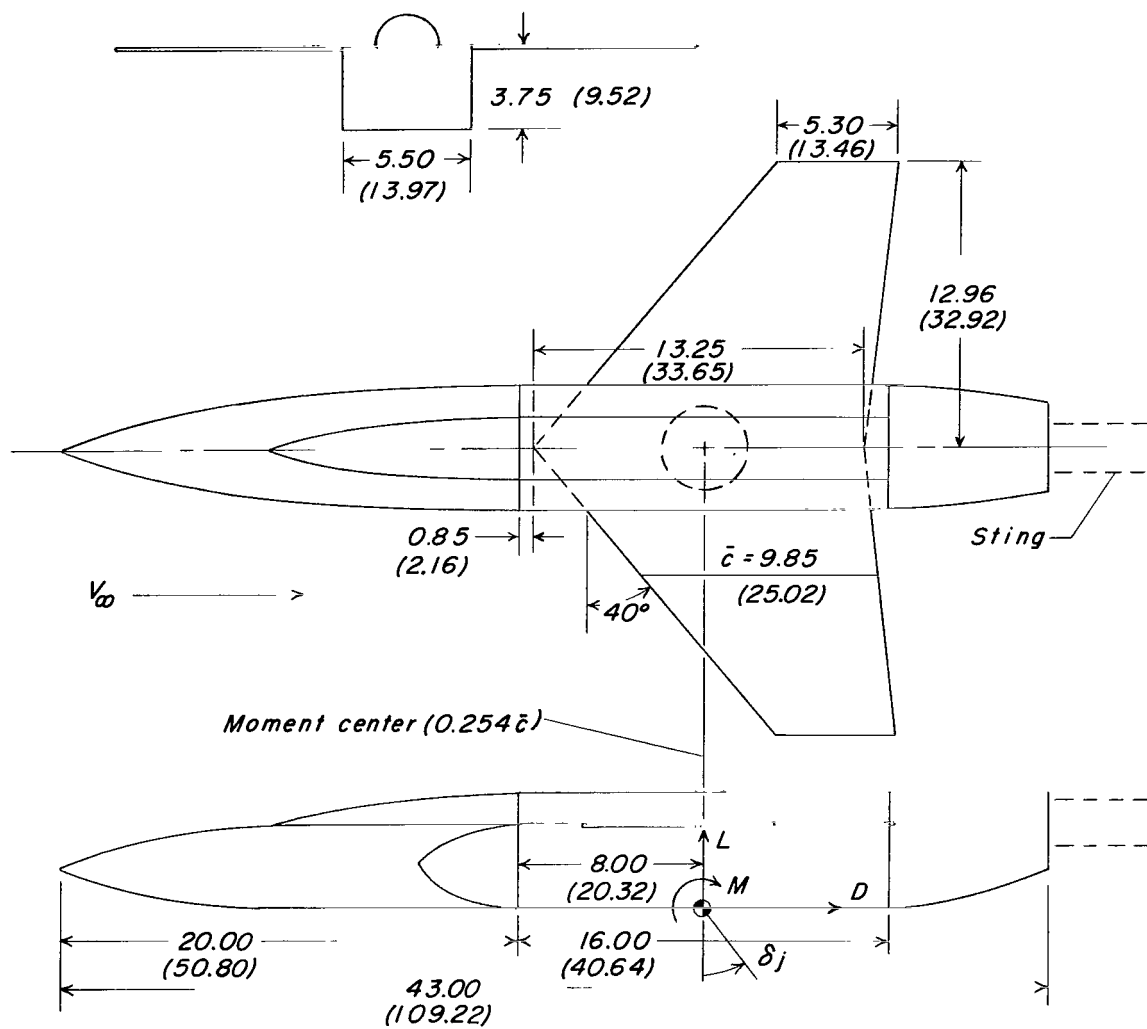


Figure 1.- Three-view drawing of model showing positive direction of forces, moments, and jet deflection angle. All dimensions are in inches (centimeters).

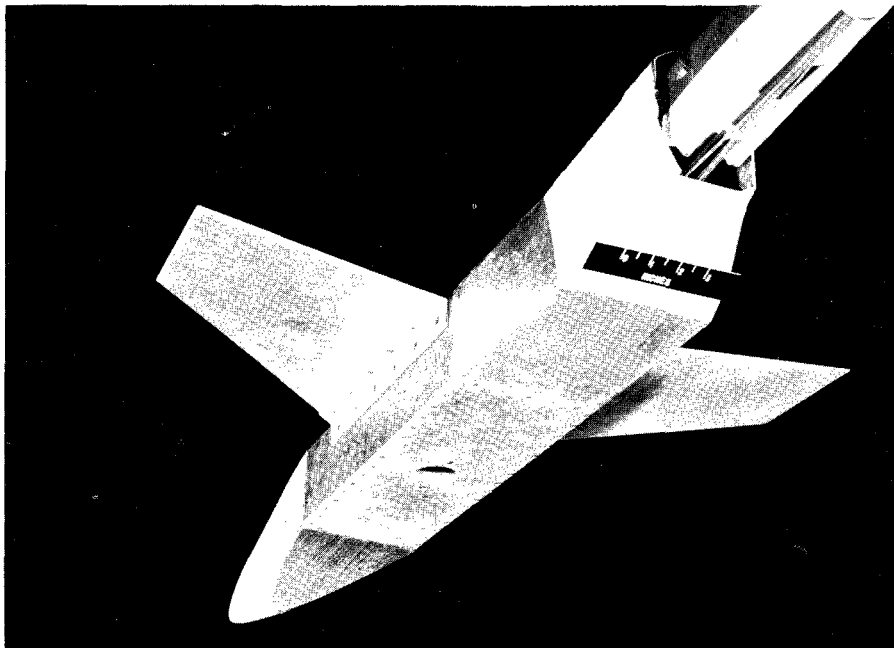


Figure 2.- Photograph of model showing a typical small round jet nozzle.

L-62-8680

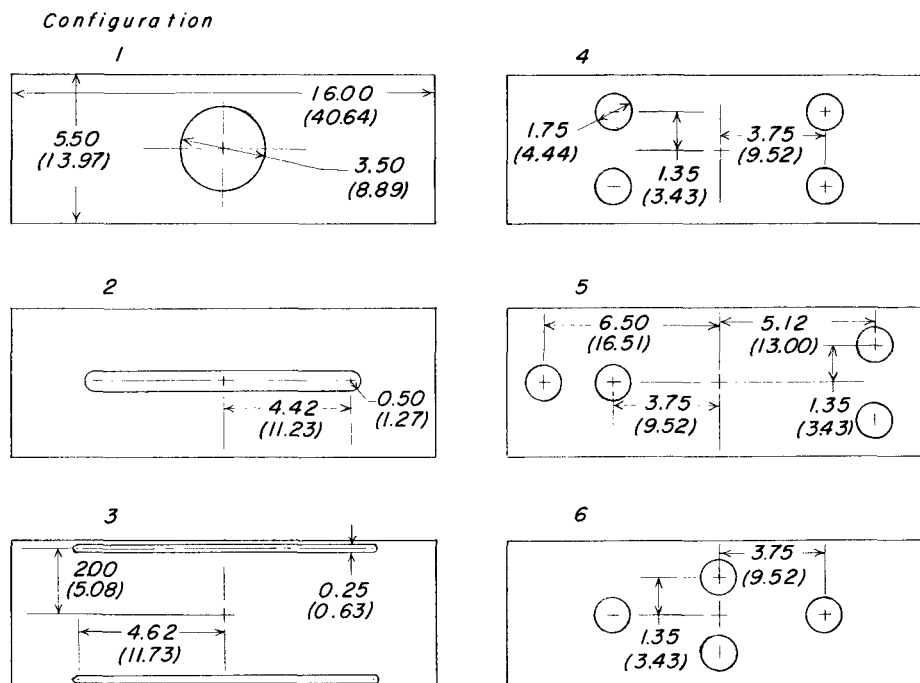


Figure 3.- Details of nozzle geometry in each removable jet configuration plate. All dimensions are in inches (centimeters).

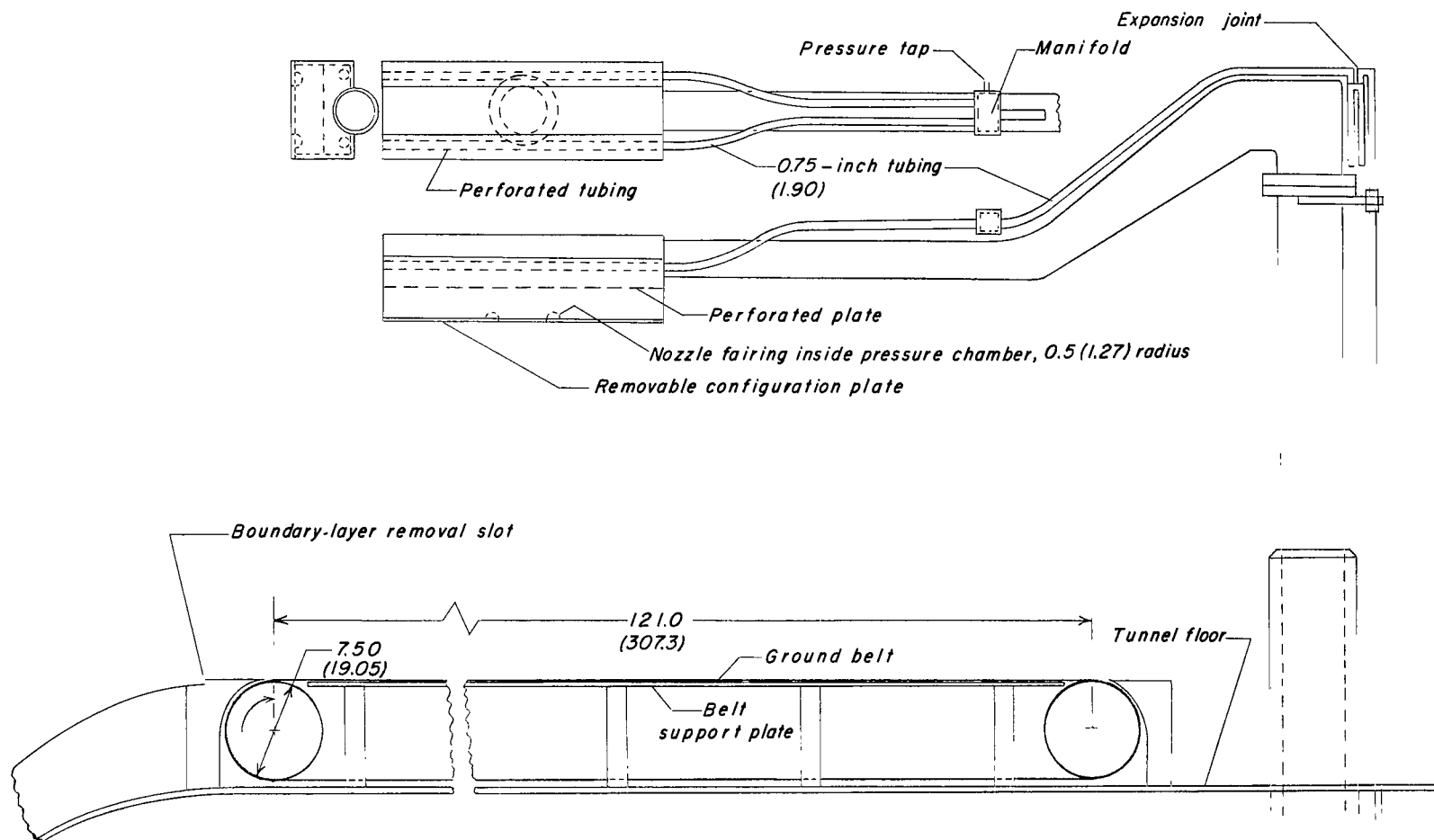


Figure 4.- Sketch showing ground belt, central part of fuselage, sting, and air line to jet nozzles, with shield over air line removed. Dimensions are in inches (centimeters).

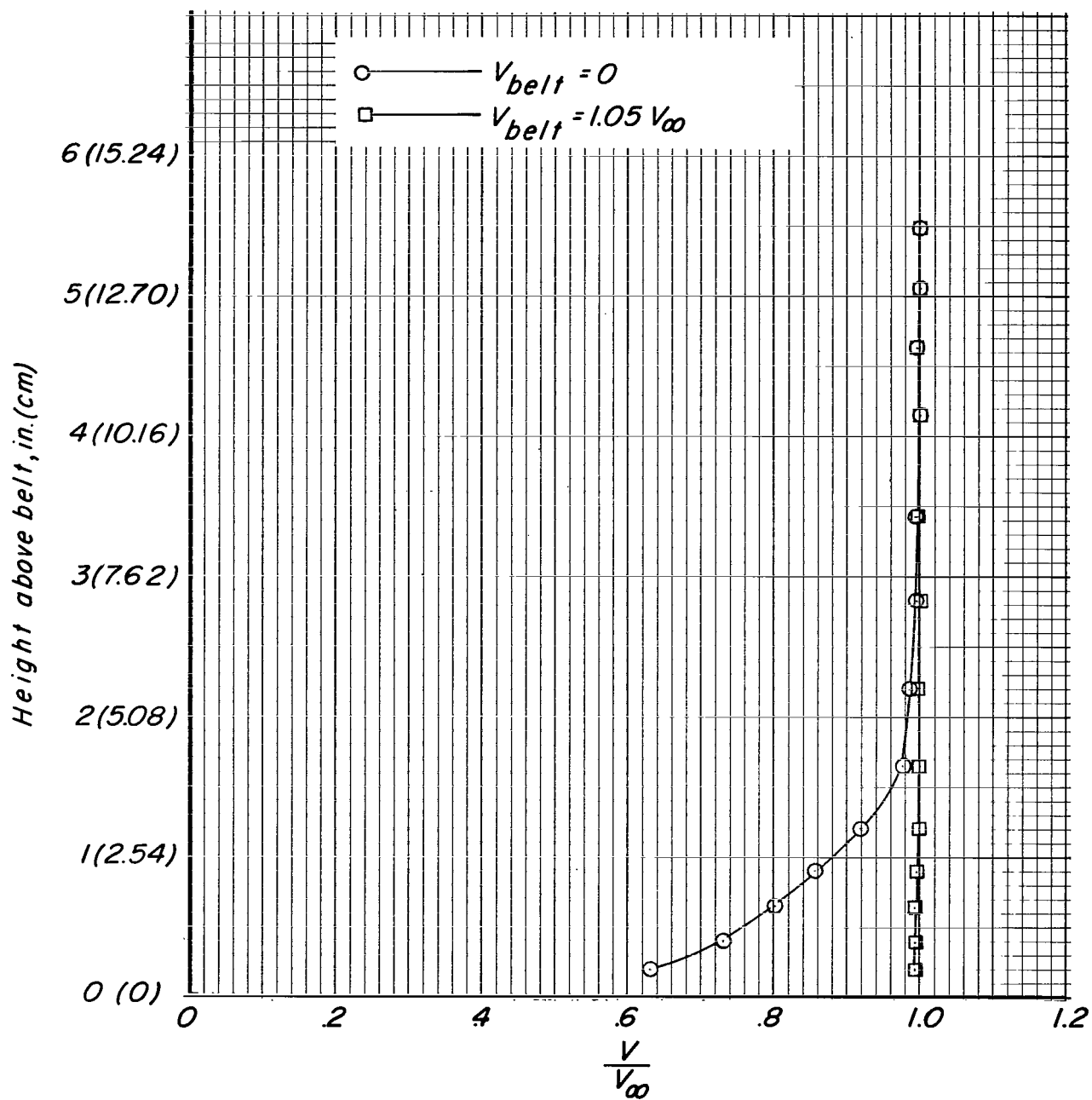
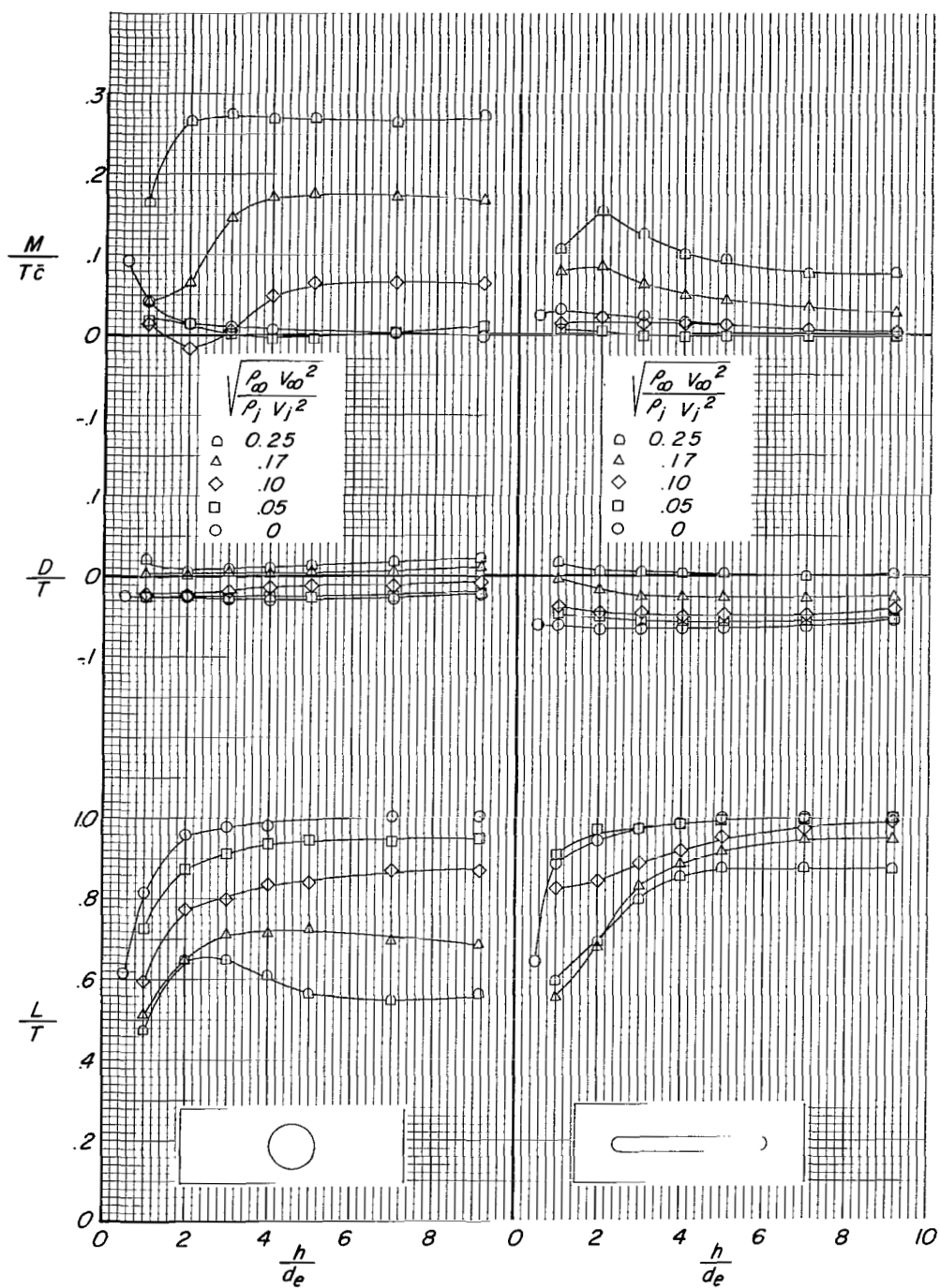
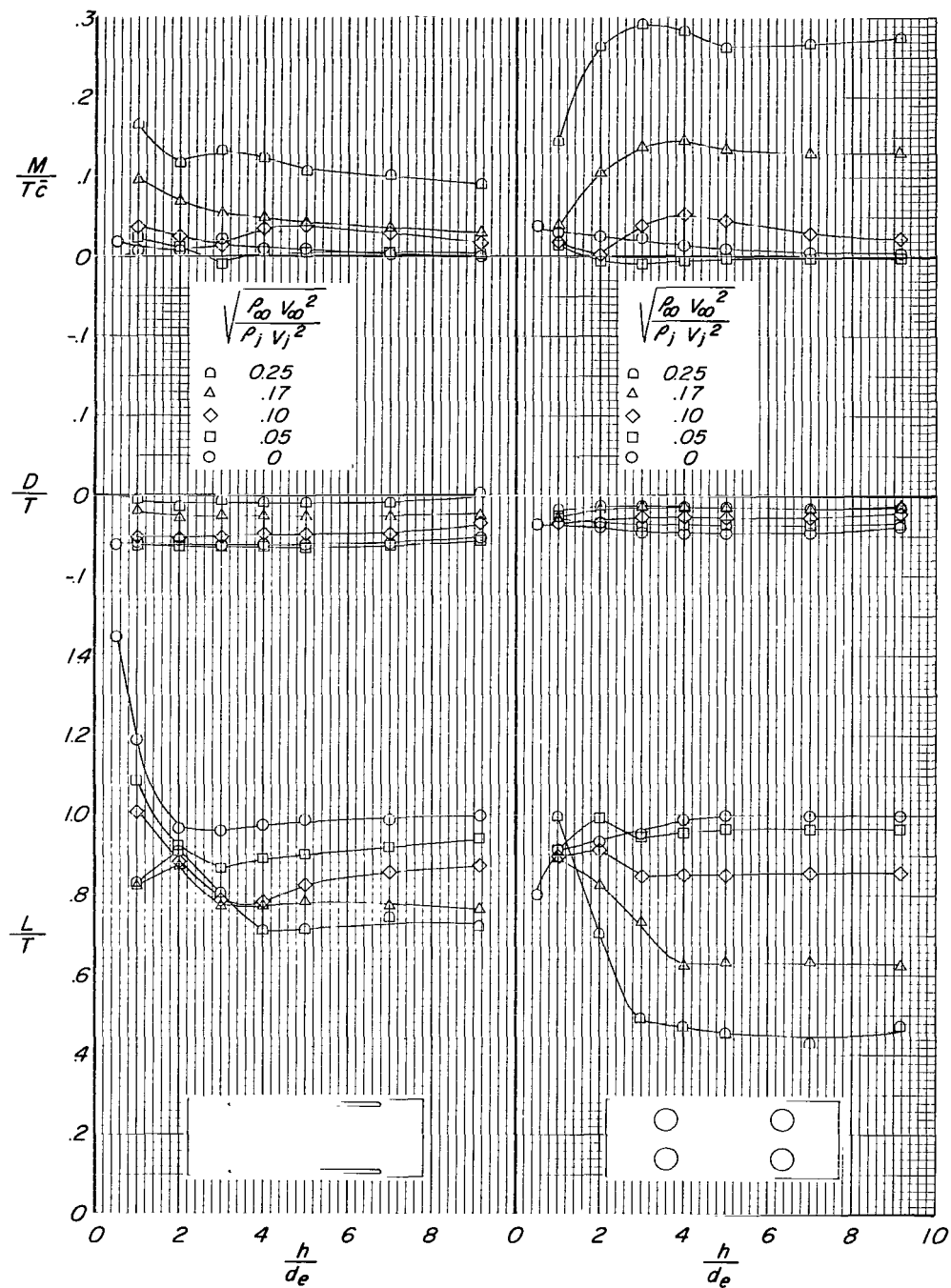


Figure 5.- Effect of moving belt on boundary-layer profile of ground plane. V is velocity in boundary layer; V_{belt} is velocity of moving belt; $V_{\infty} = 82.5 \text{ ft/s (25.14 m/s)}$.



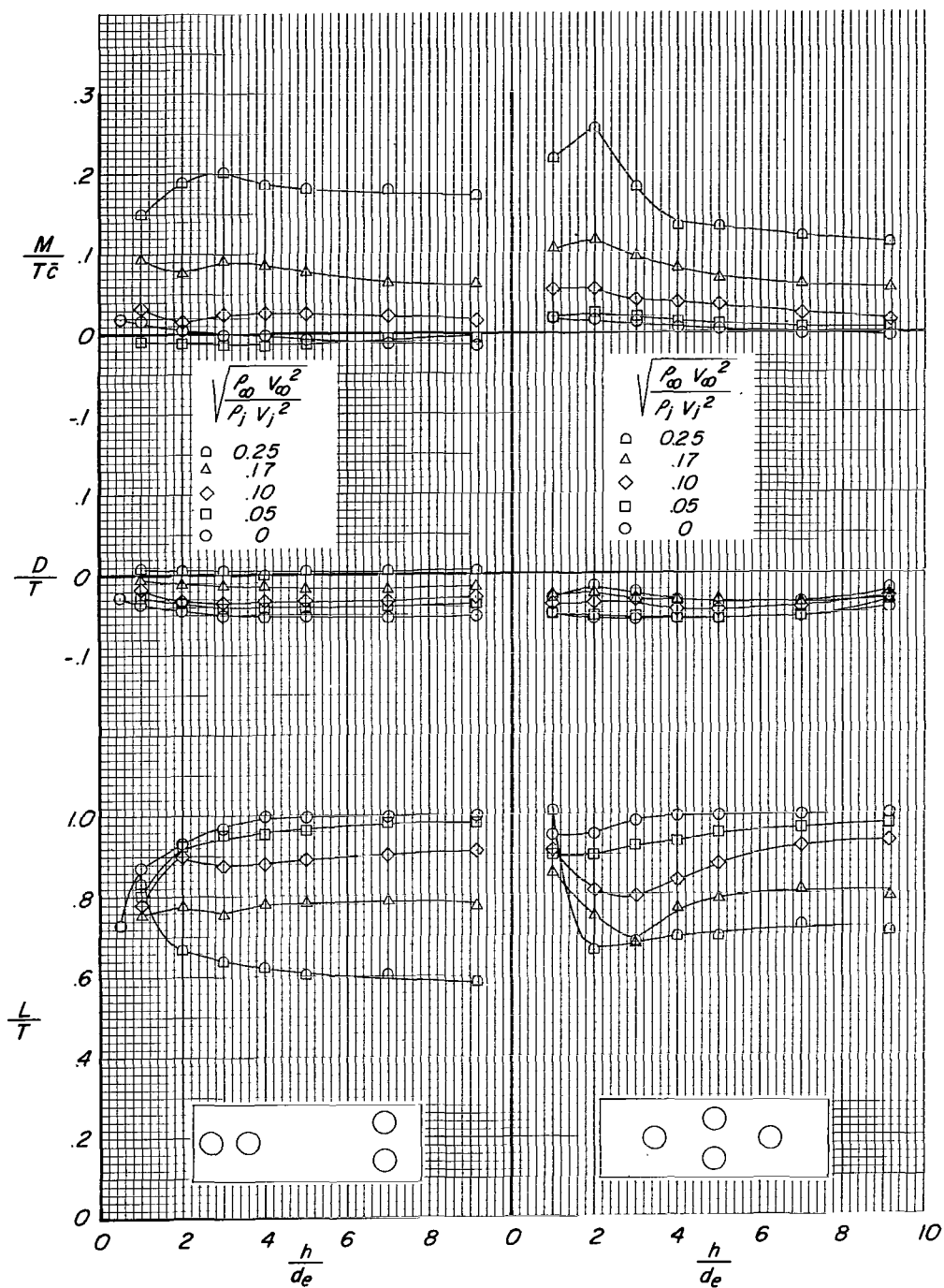
(a) Configurations 1 and 2.

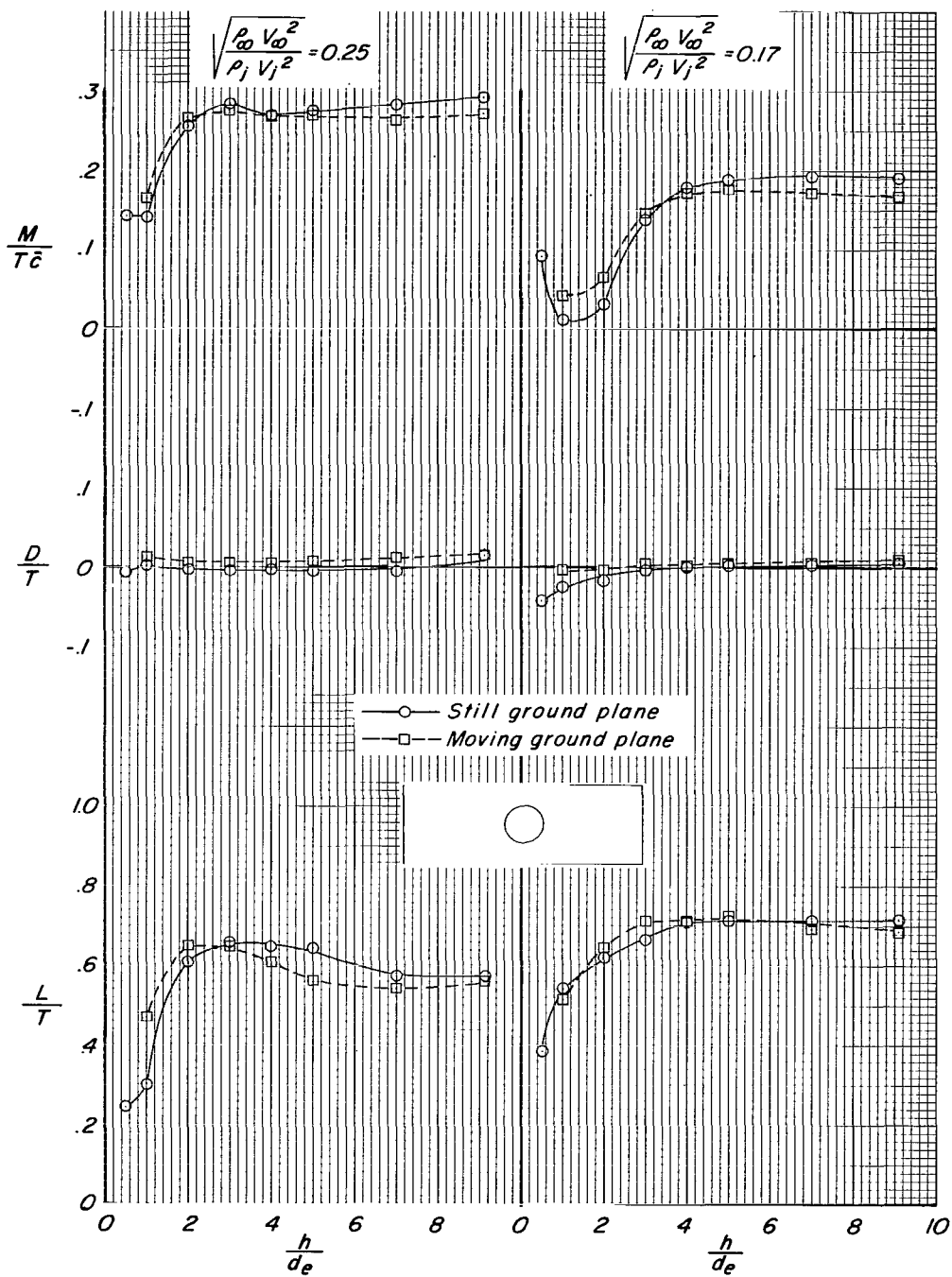
Figure 6.- Longitudinal characteristics of model configurations in moving-ground-plane effect for various forward speeds and thrust conditions.
 $\alpha = 0^\circ$.



(b) Configurations 3 and 4.

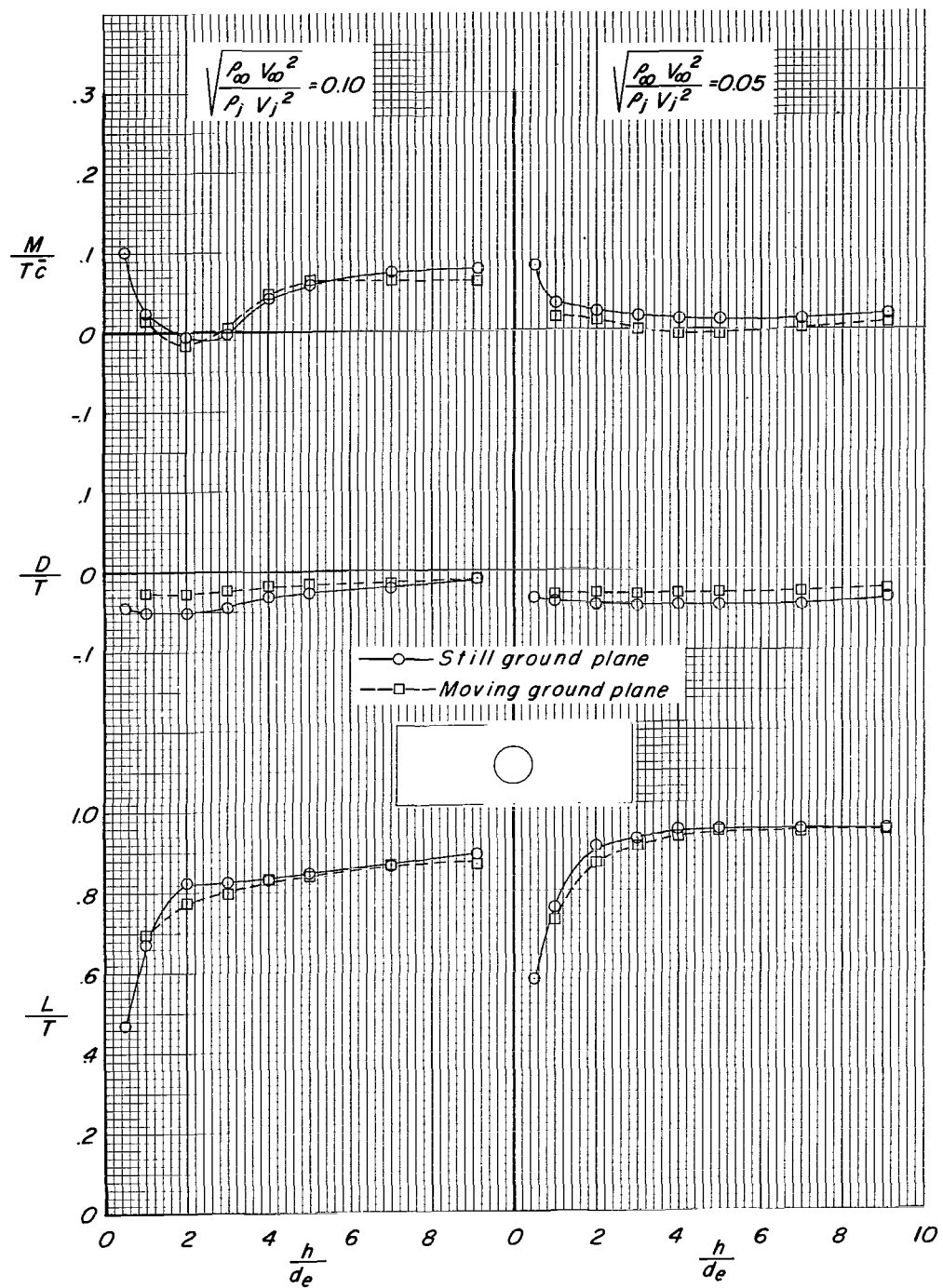
Figure 6.- Continued.





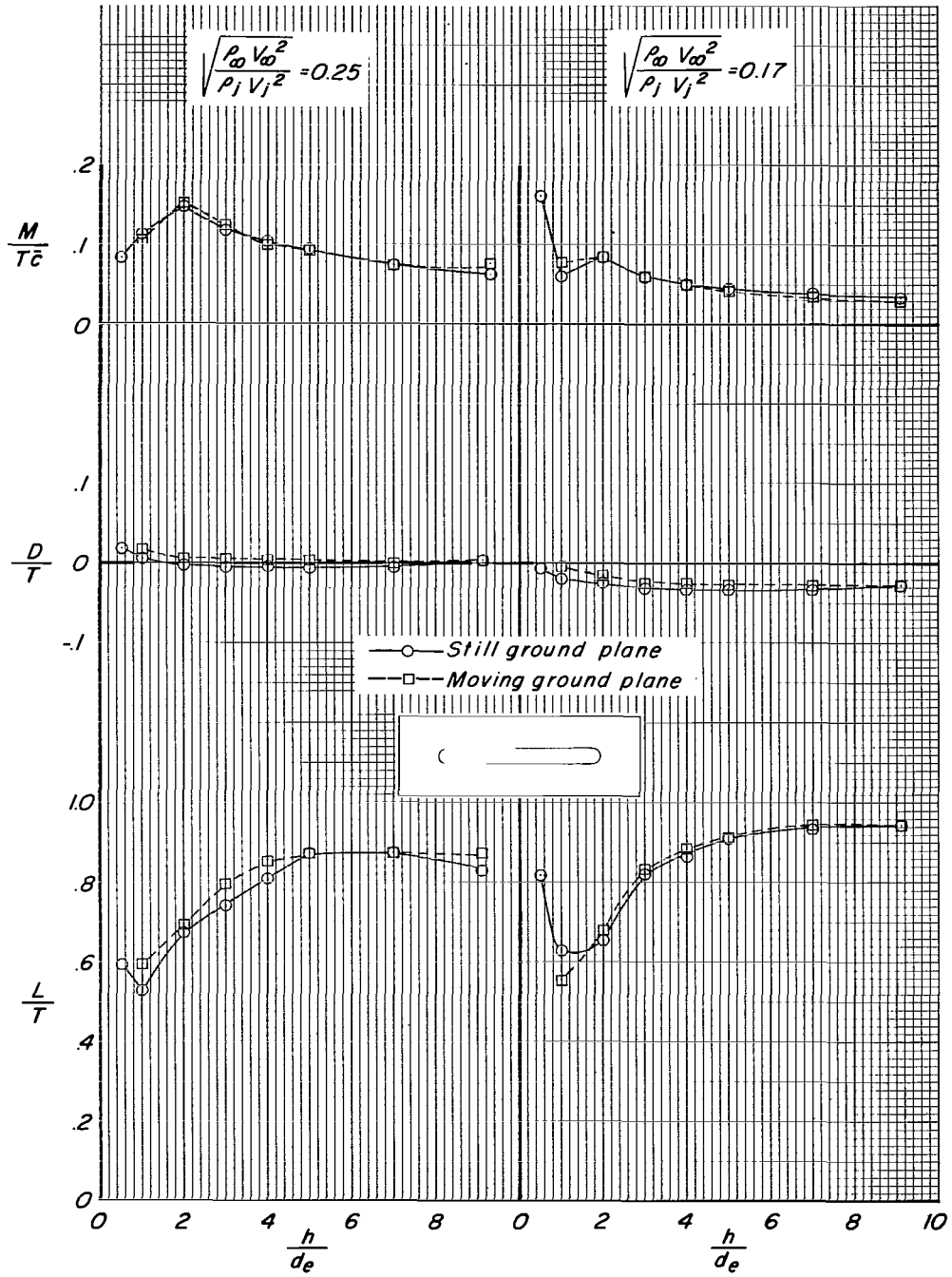
(a) Configuration 1.

Figure 7.- Comparison of effects of a still and a moving ground plane for various forward speeds and thrust conditions through a range of model heights at $\alpha = 0^\circ$.



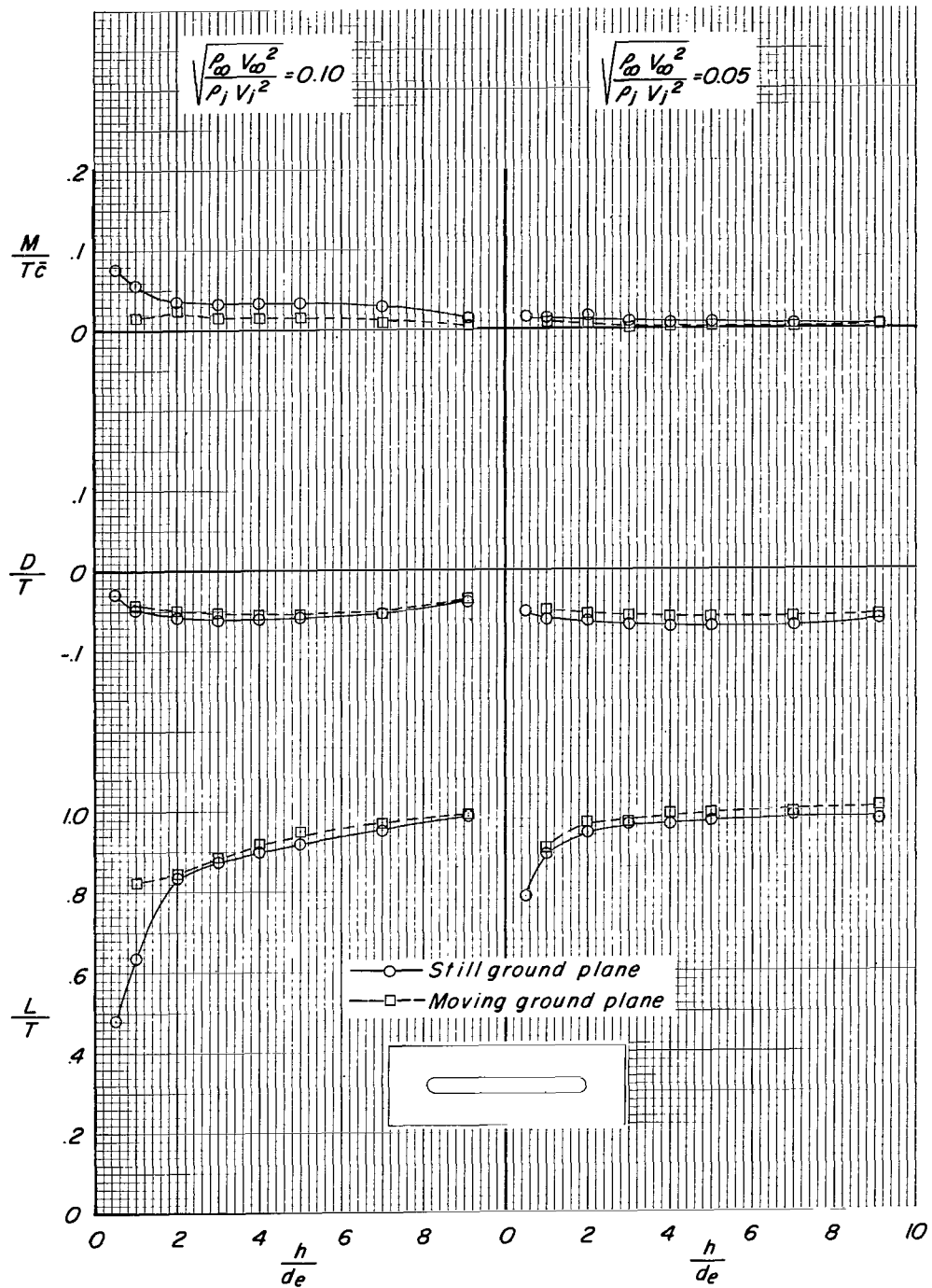
(a) Concluded.

Figure 7.- Continued.



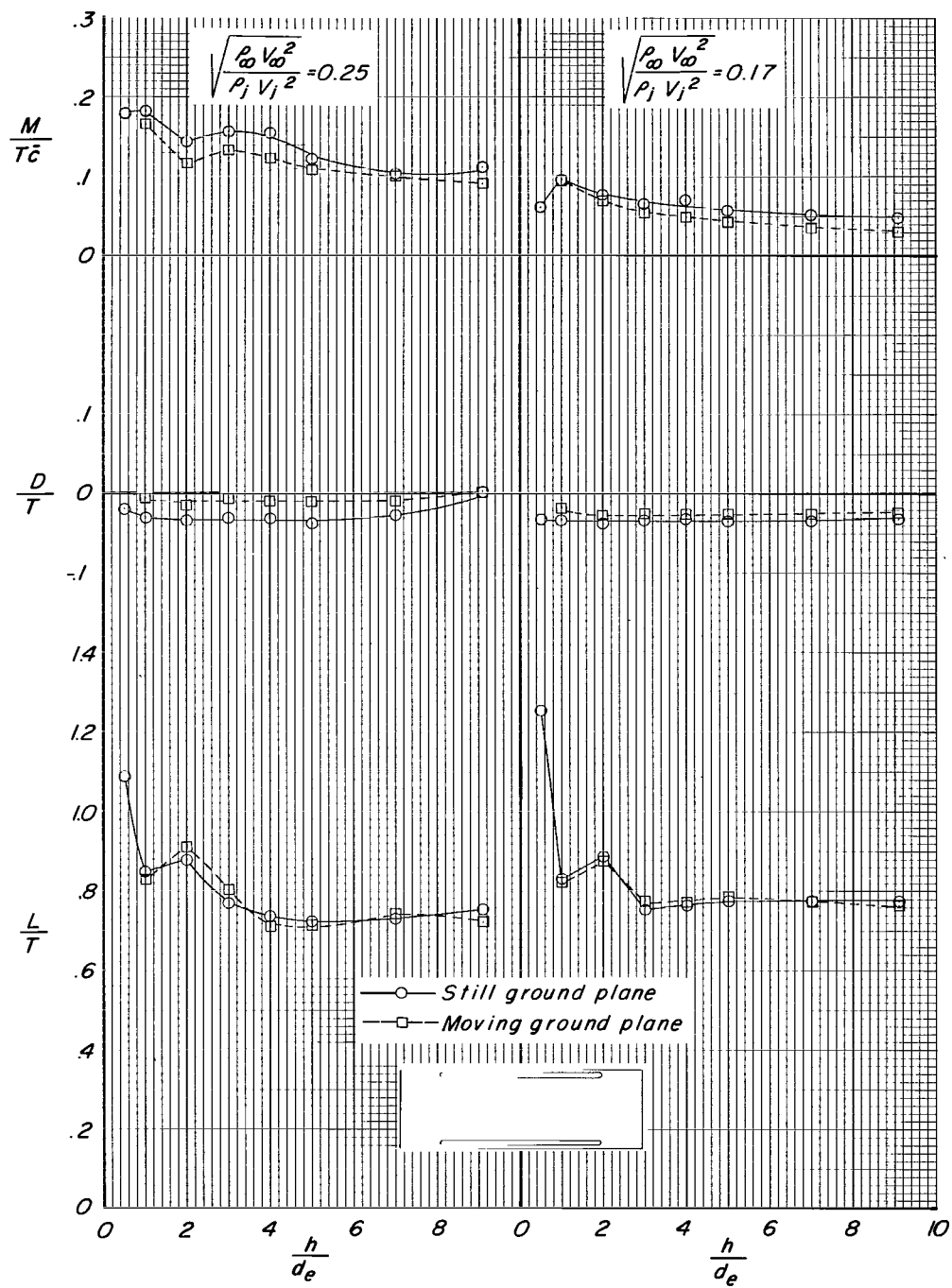
(b) Configuration 2.

Figure 7.- Continued.



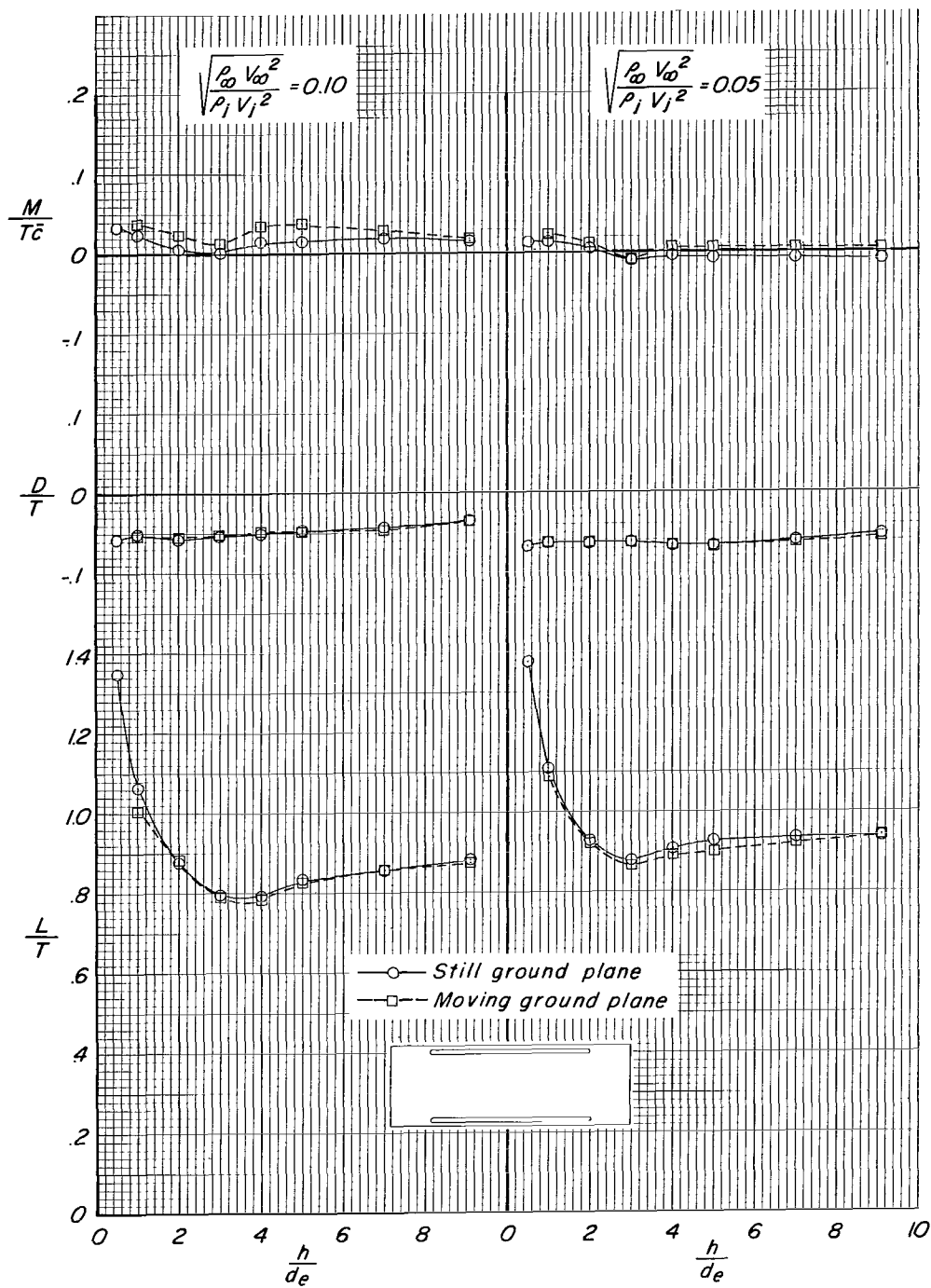
(b) Concluded.

Figure 7.- Continued.



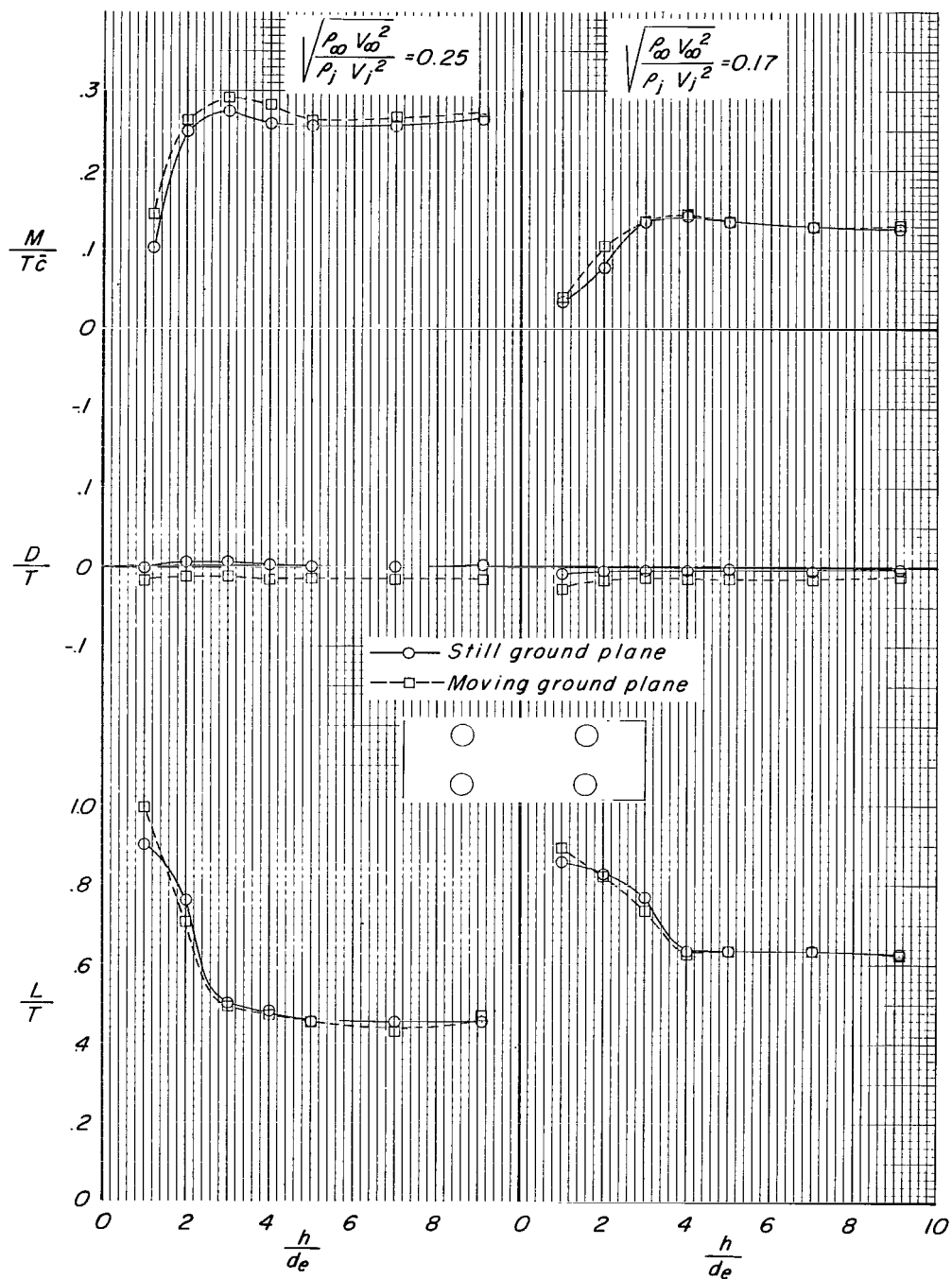
(c) Configuration 3.

Figure 7.- Continued.



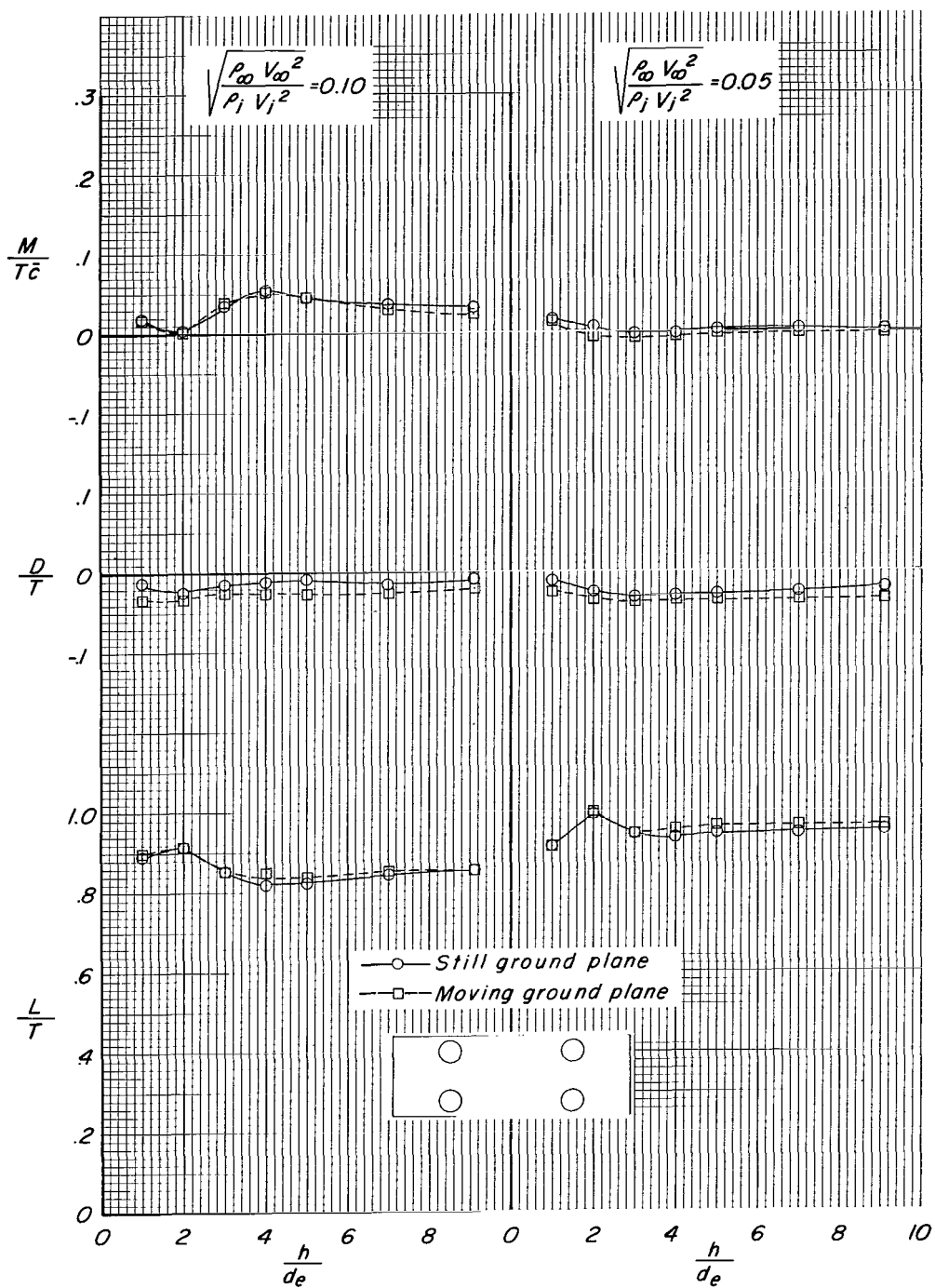
(c) Concluded.

Figure 7.- Continued.



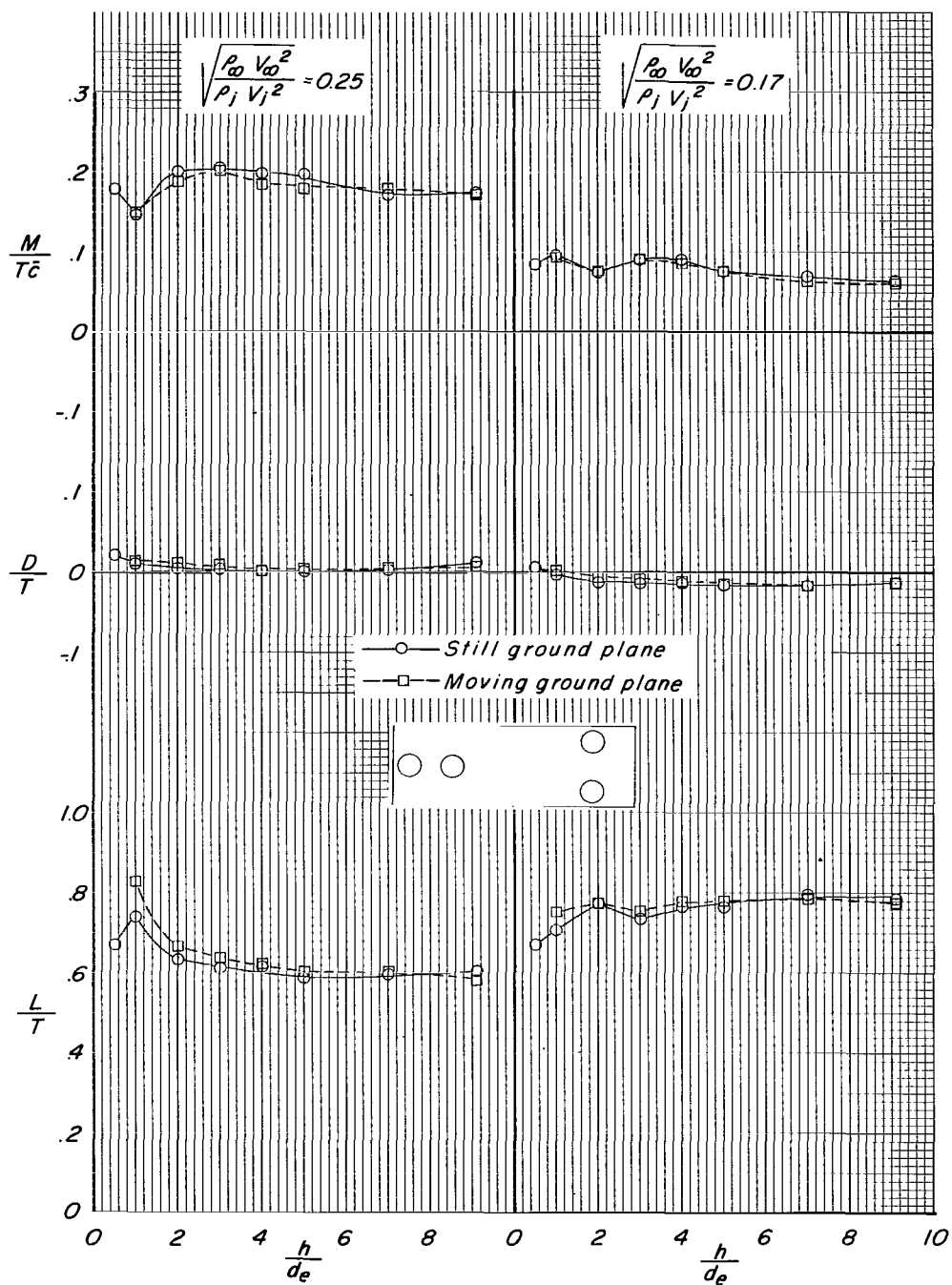
(d) Configuration 4.

Figure 7.- Continued.



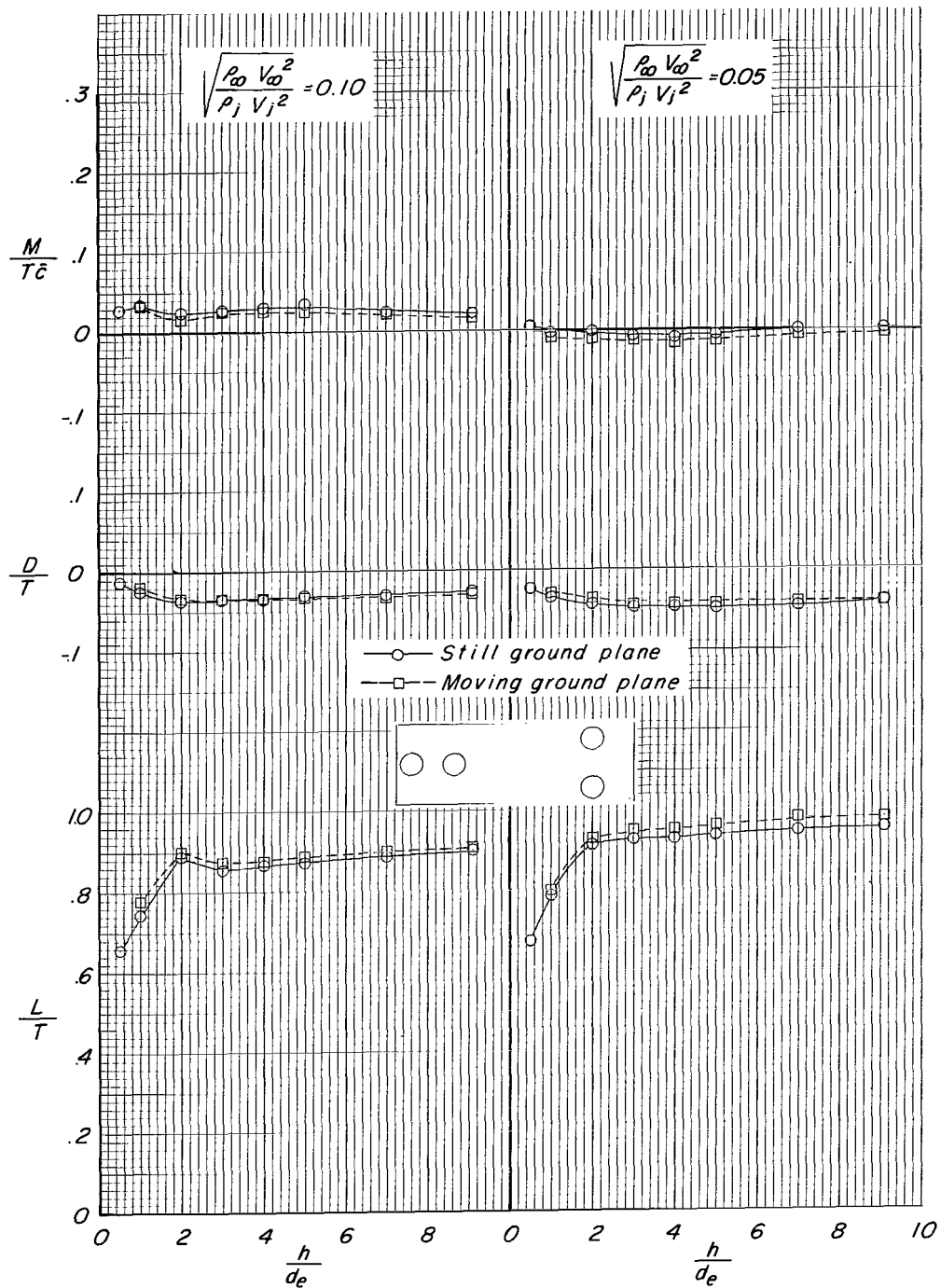
(d) Concluded.

Figure 7.- Continued.



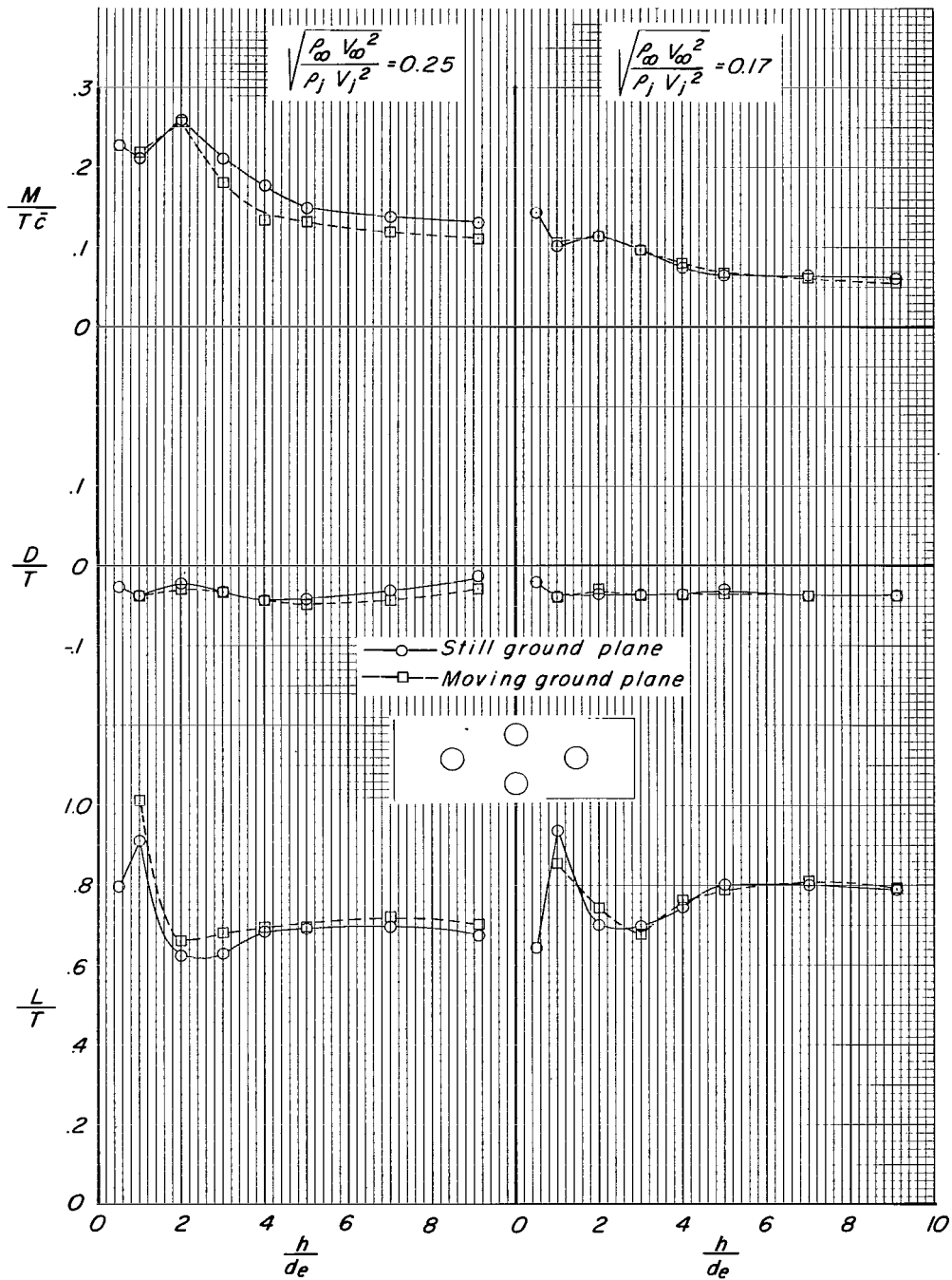
(e) Configuration 5.

Figure 7.- Continued.



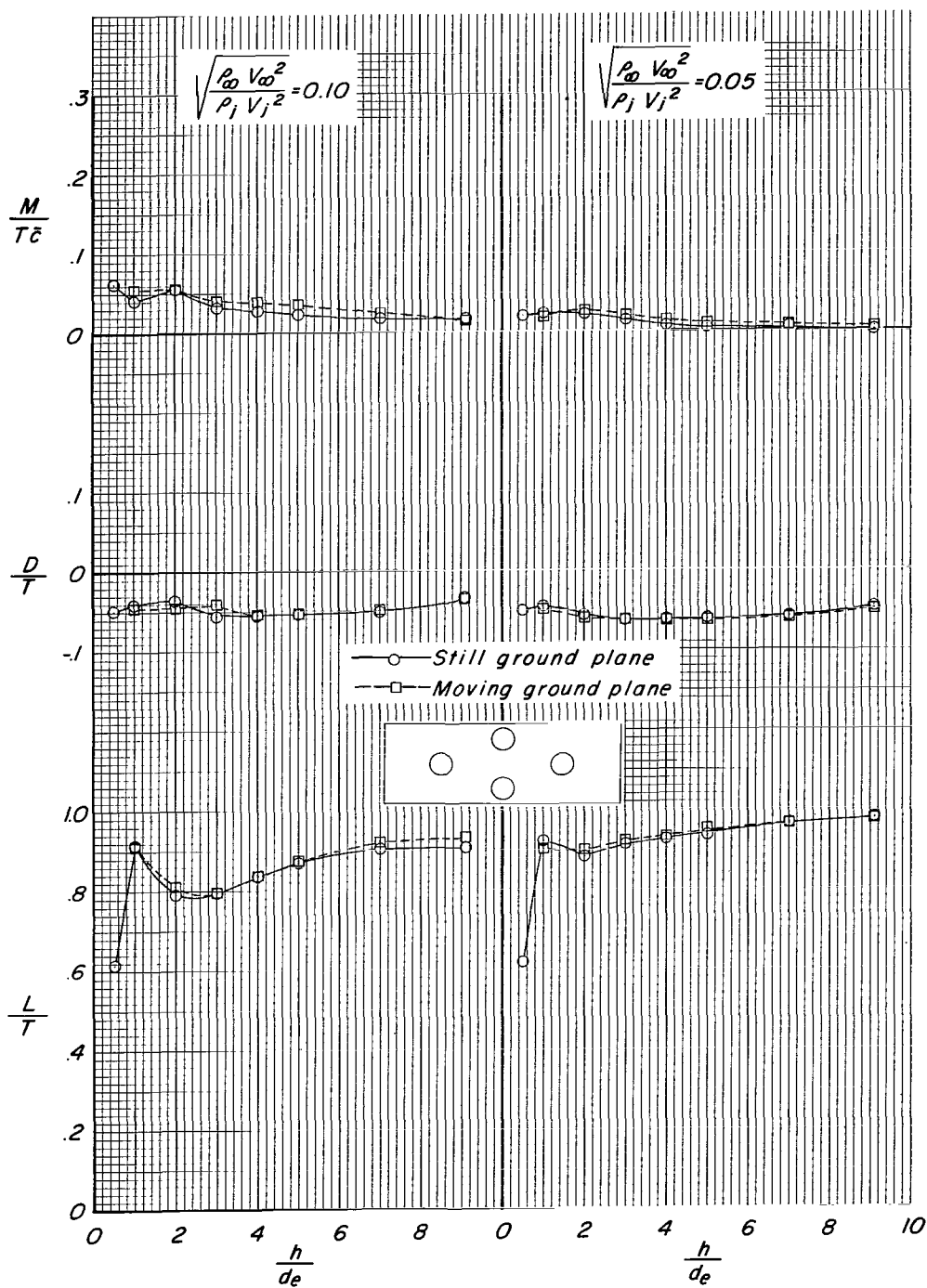
(e) Concluded.

Figure 7.- Continued.



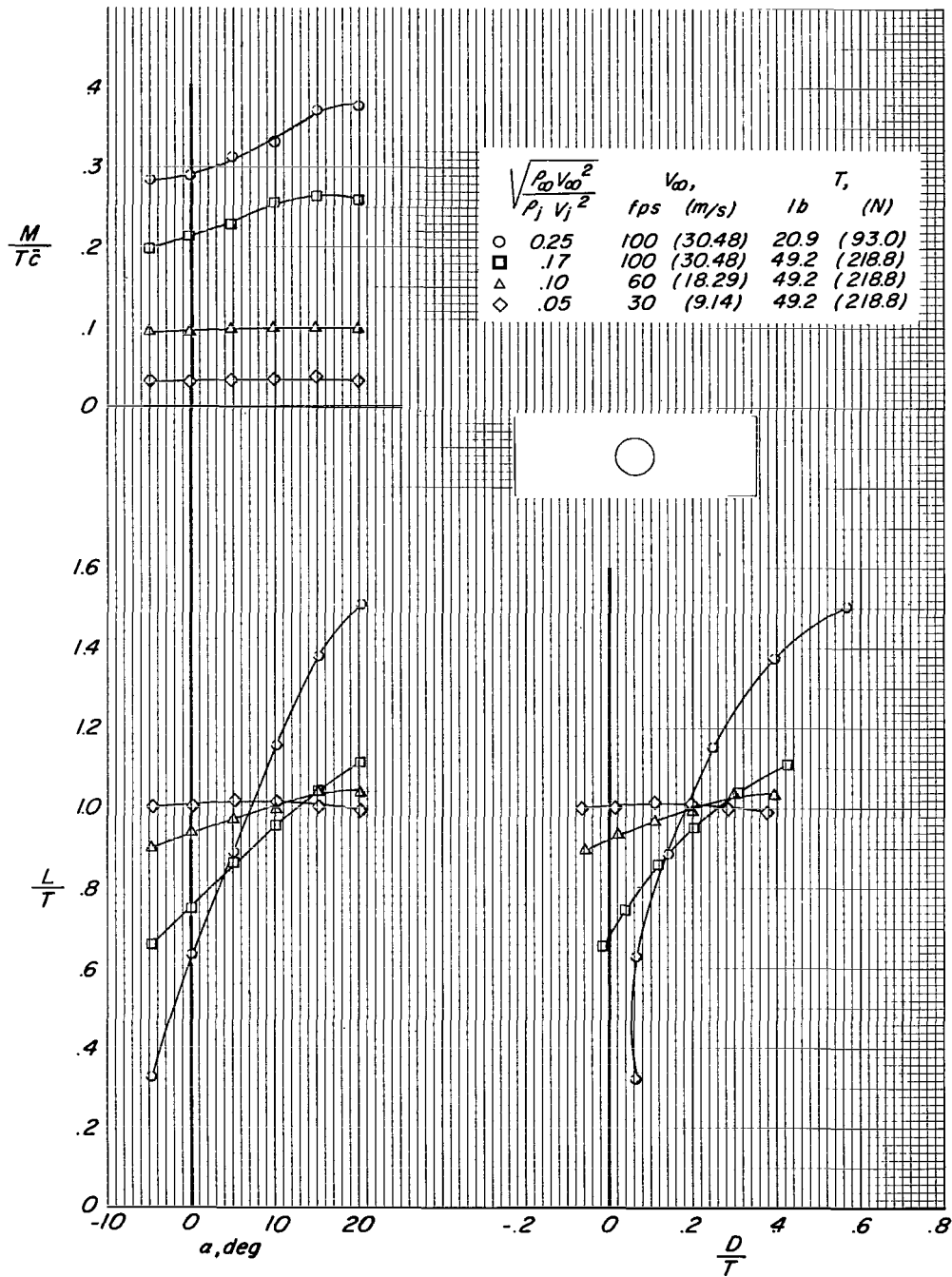
(f) Configuration 6.

Figure 7.- Continued.



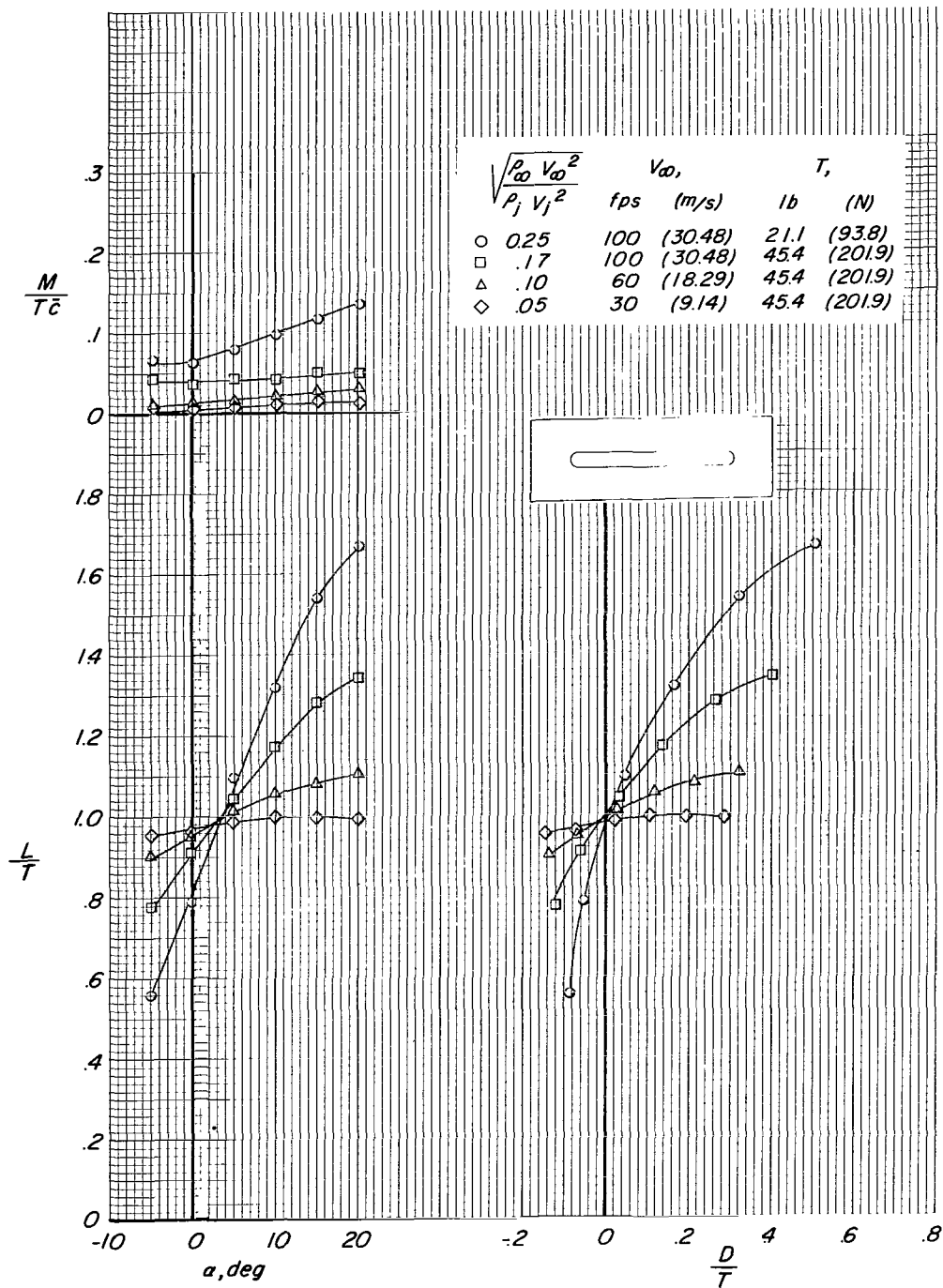
(f) Concluded.

Figure 7.- Concluded.



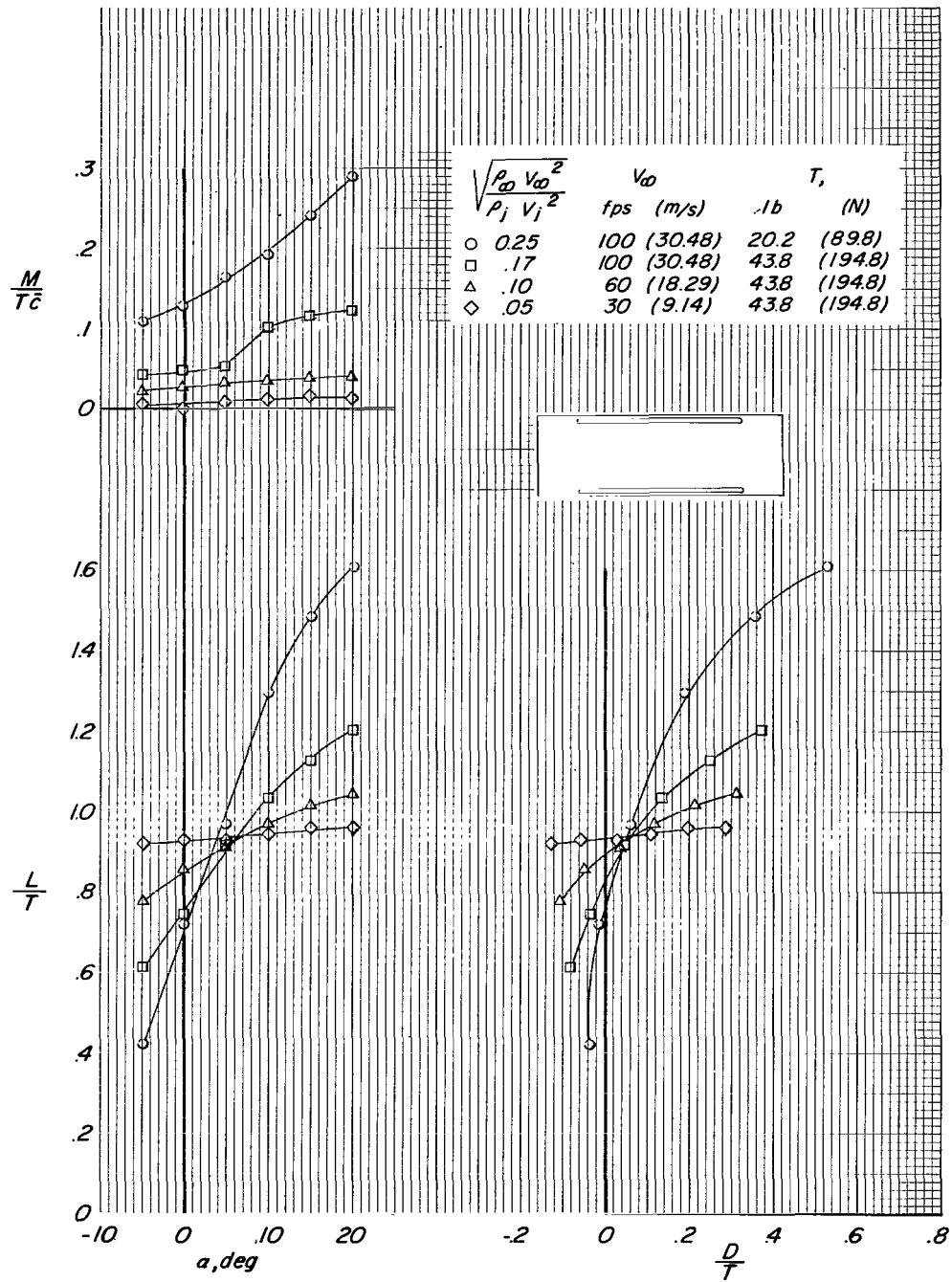
(a) Configuration 1.

Figure 8.- Longitudinal characteristics of model configurations out of ground effect for various forward speeds and thrust conditions.



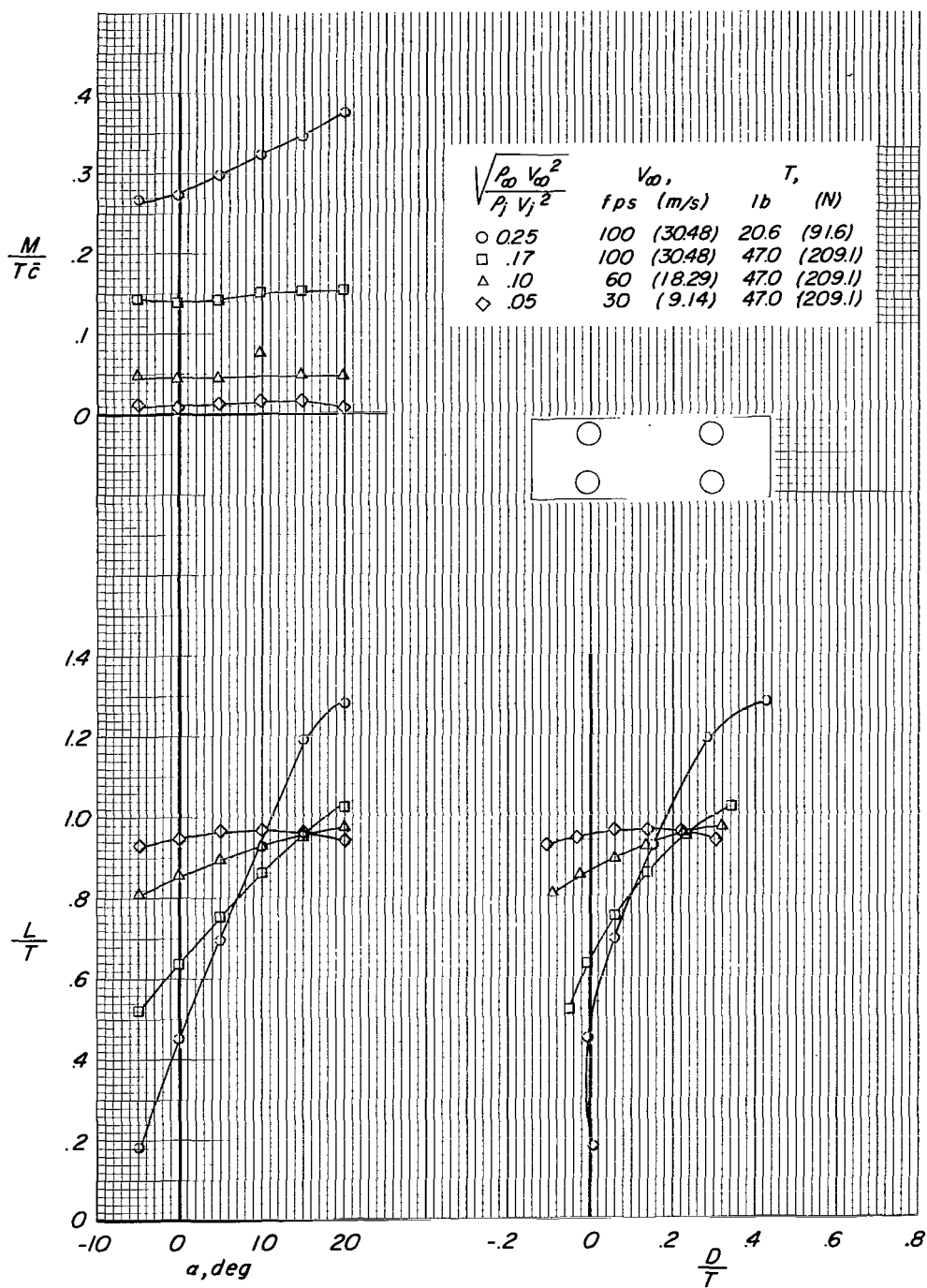
(b) Configuration 2.

Figure 8.- Continued.



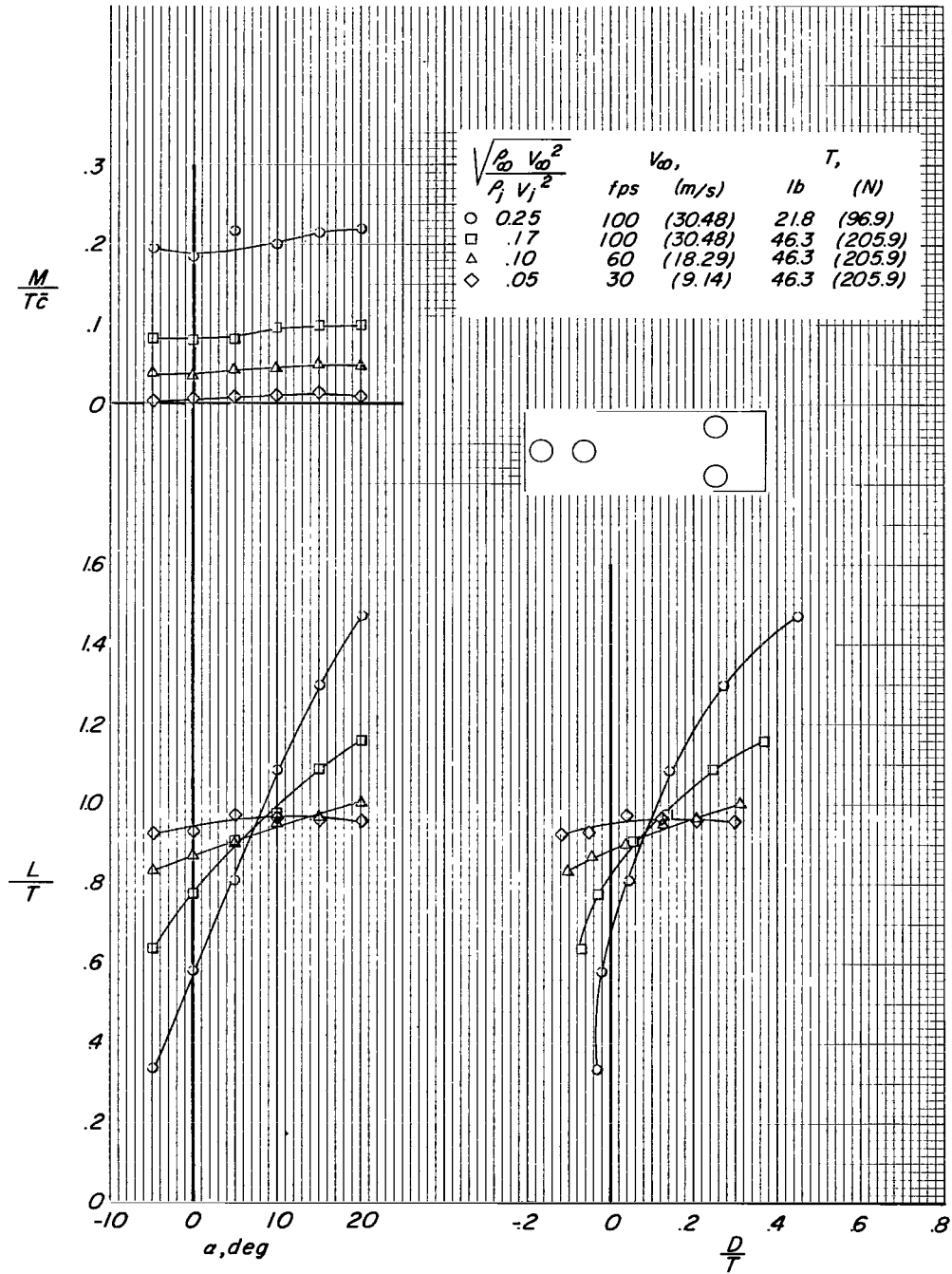
(c) Configuration 3.

Figure 8.- Continued.



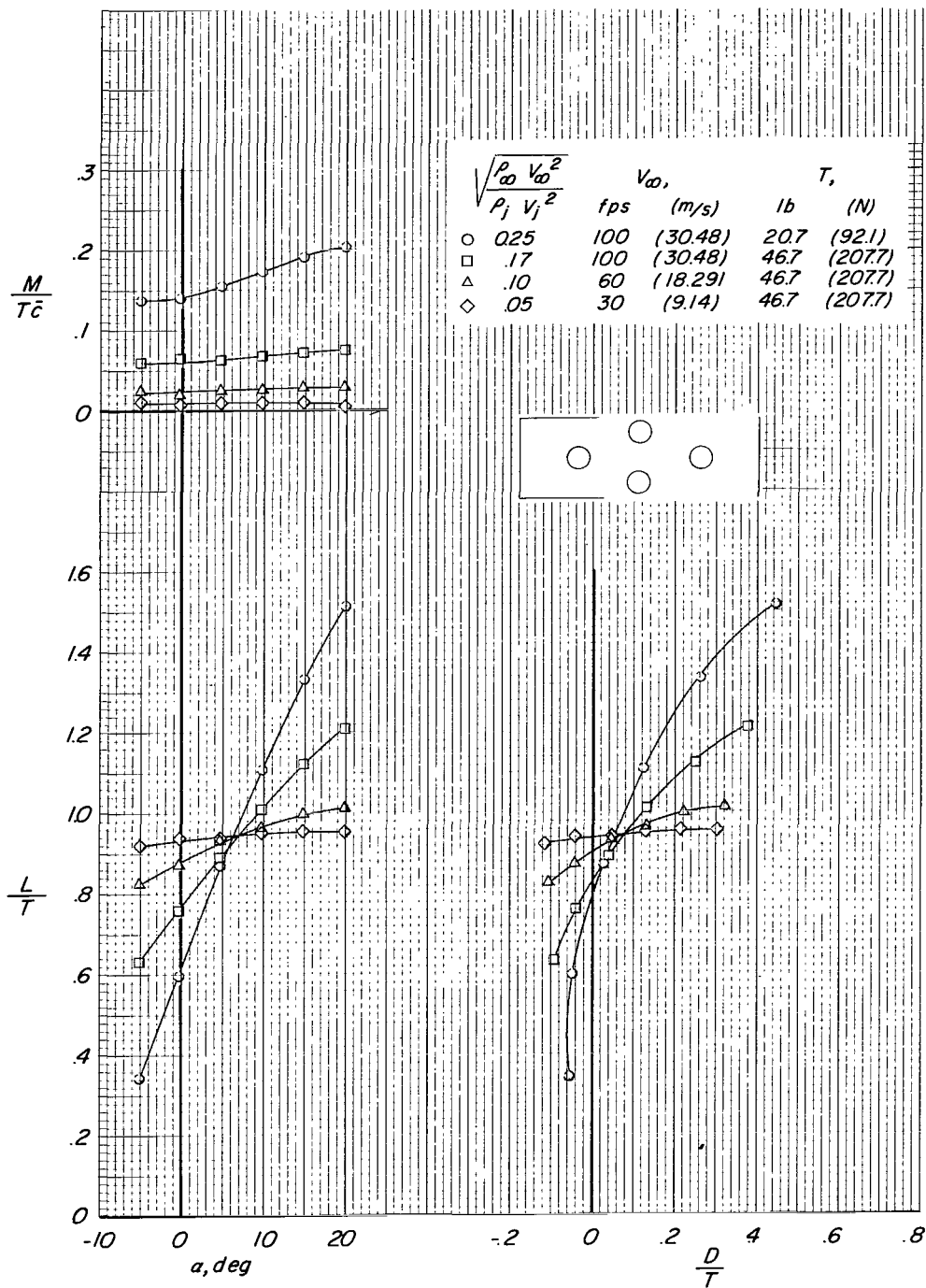
(d) Configuration 4.

Figure 8.- Continued.



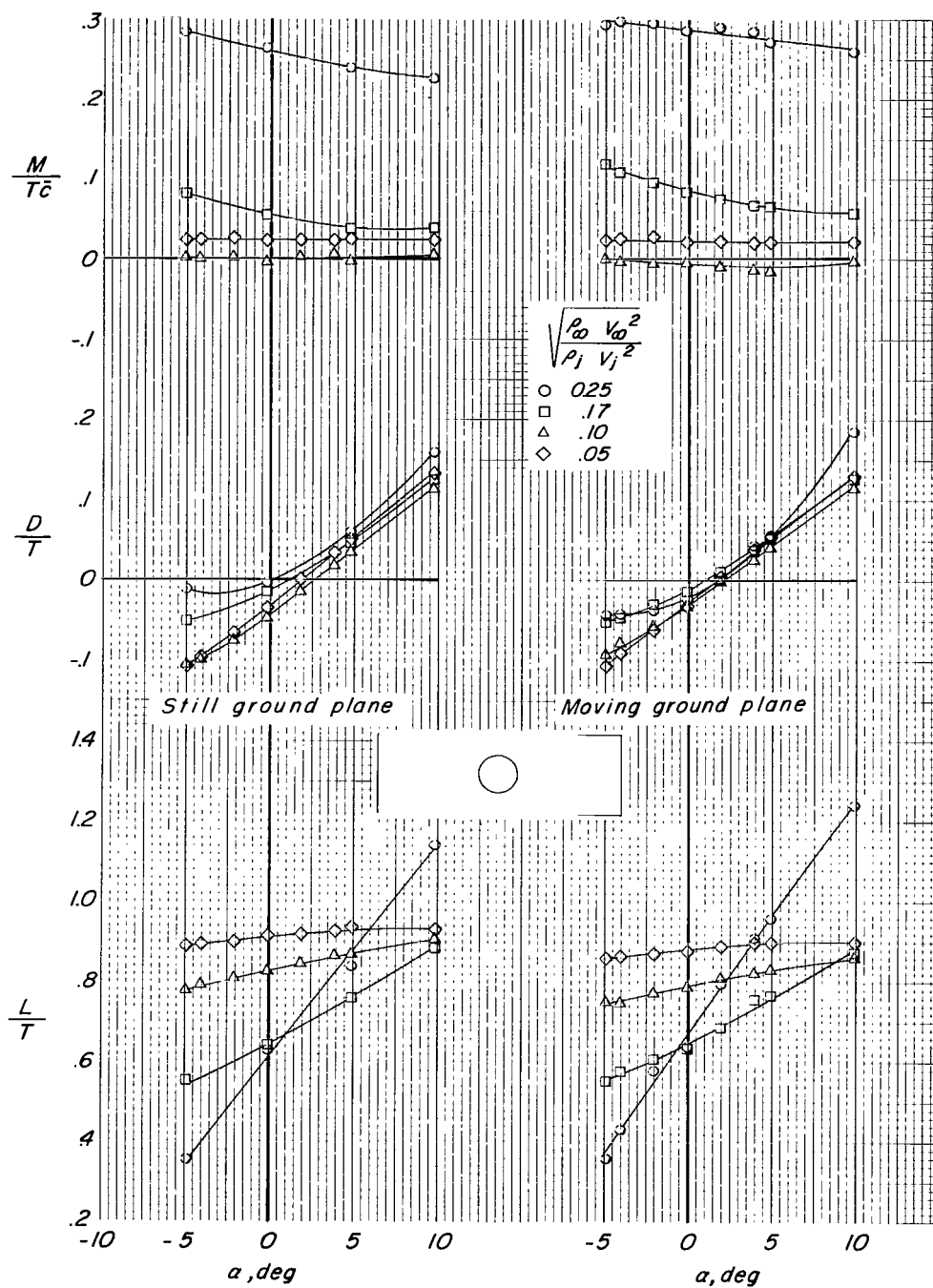
(e) Configuration 5.

Figure 8.- Continued.



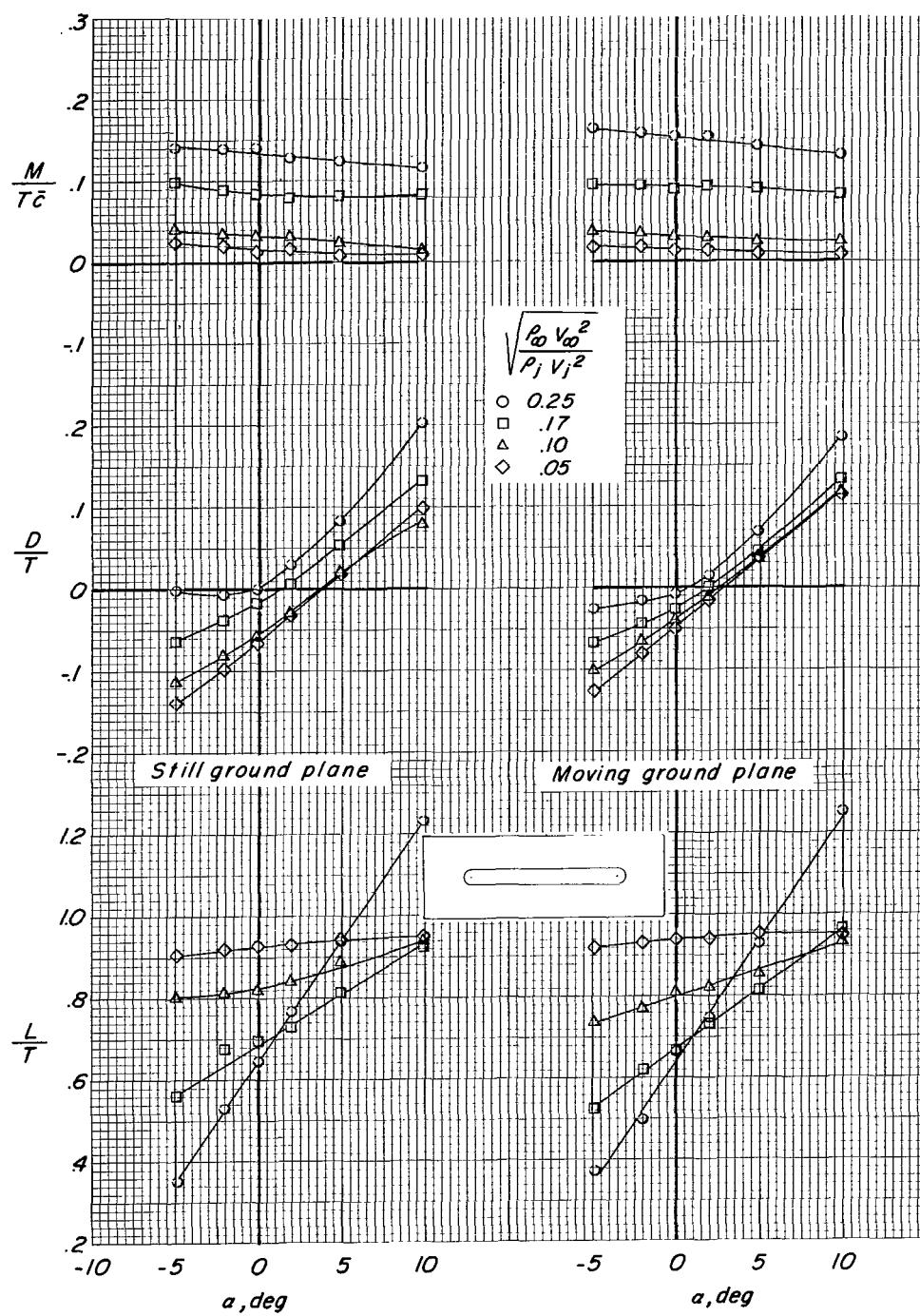
(f) Configuration 6.

Figure 8.- Concluded.



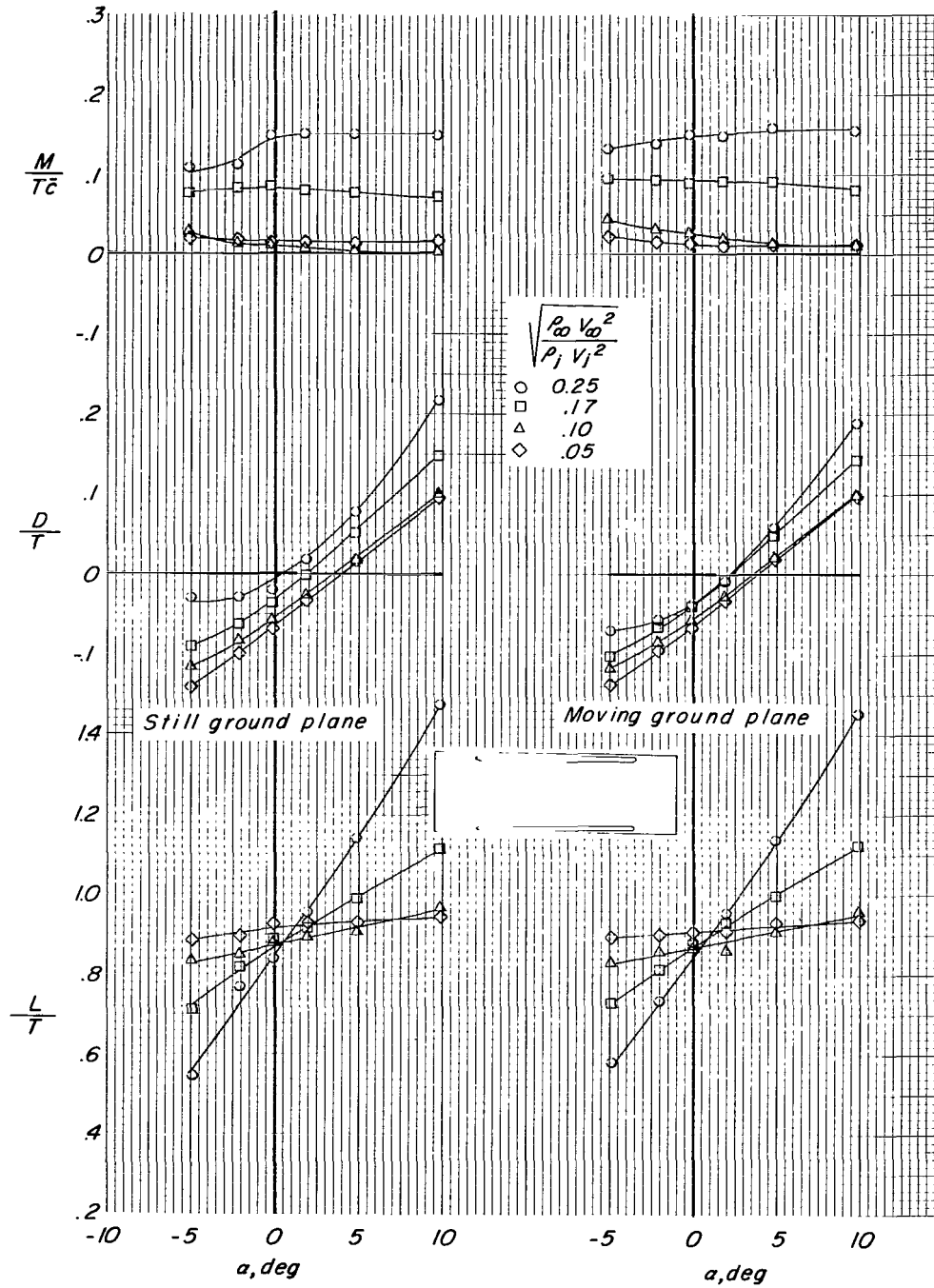
(a) Configuration 1.

Figure 9.- Longitudinal characteristics of model configurations through an angle-of-attack range at a height of 2 effective nozzle diameters from a still and a moving ground plane.



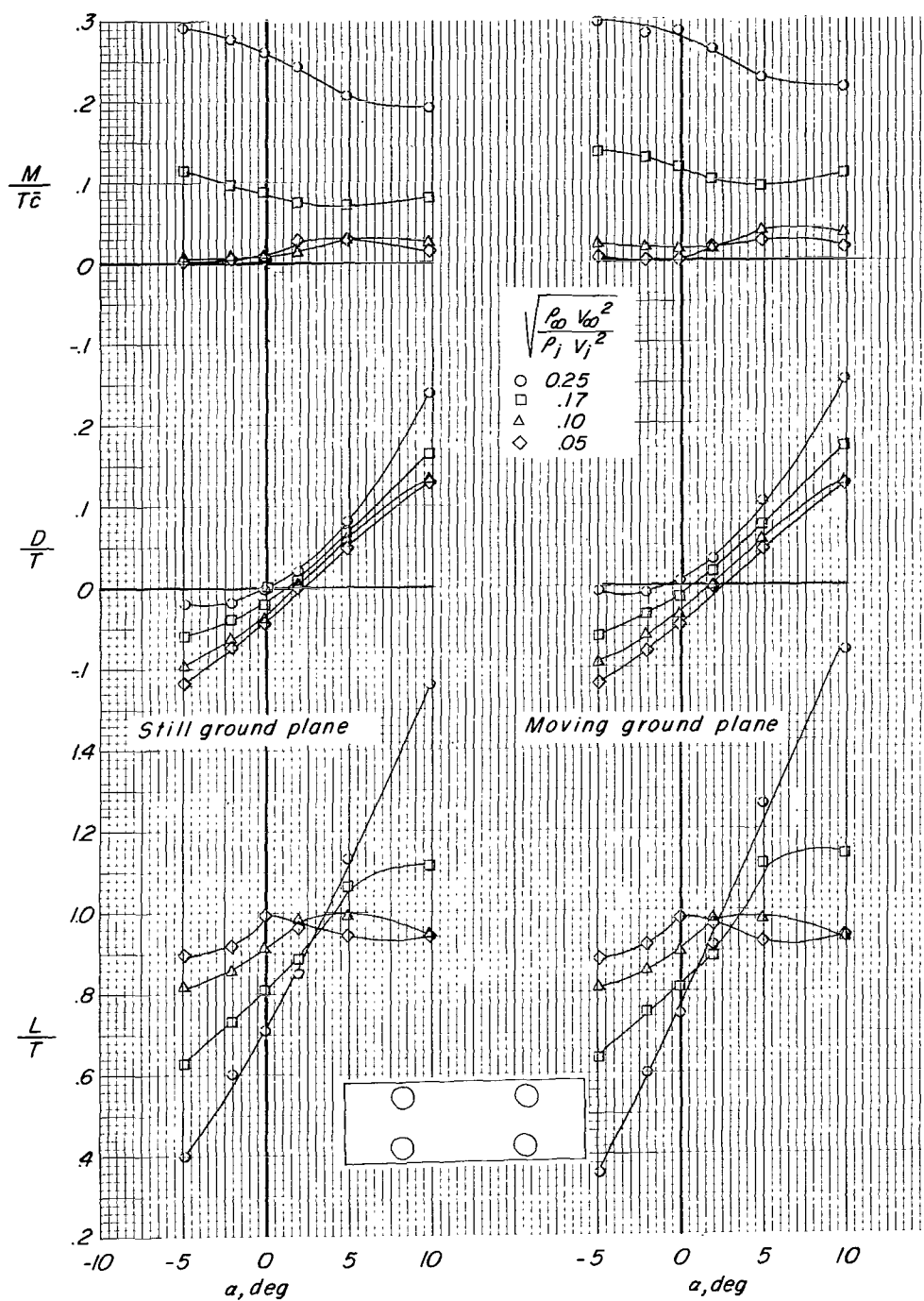
(b) Configuration 2.

Figure 9.- Continued.



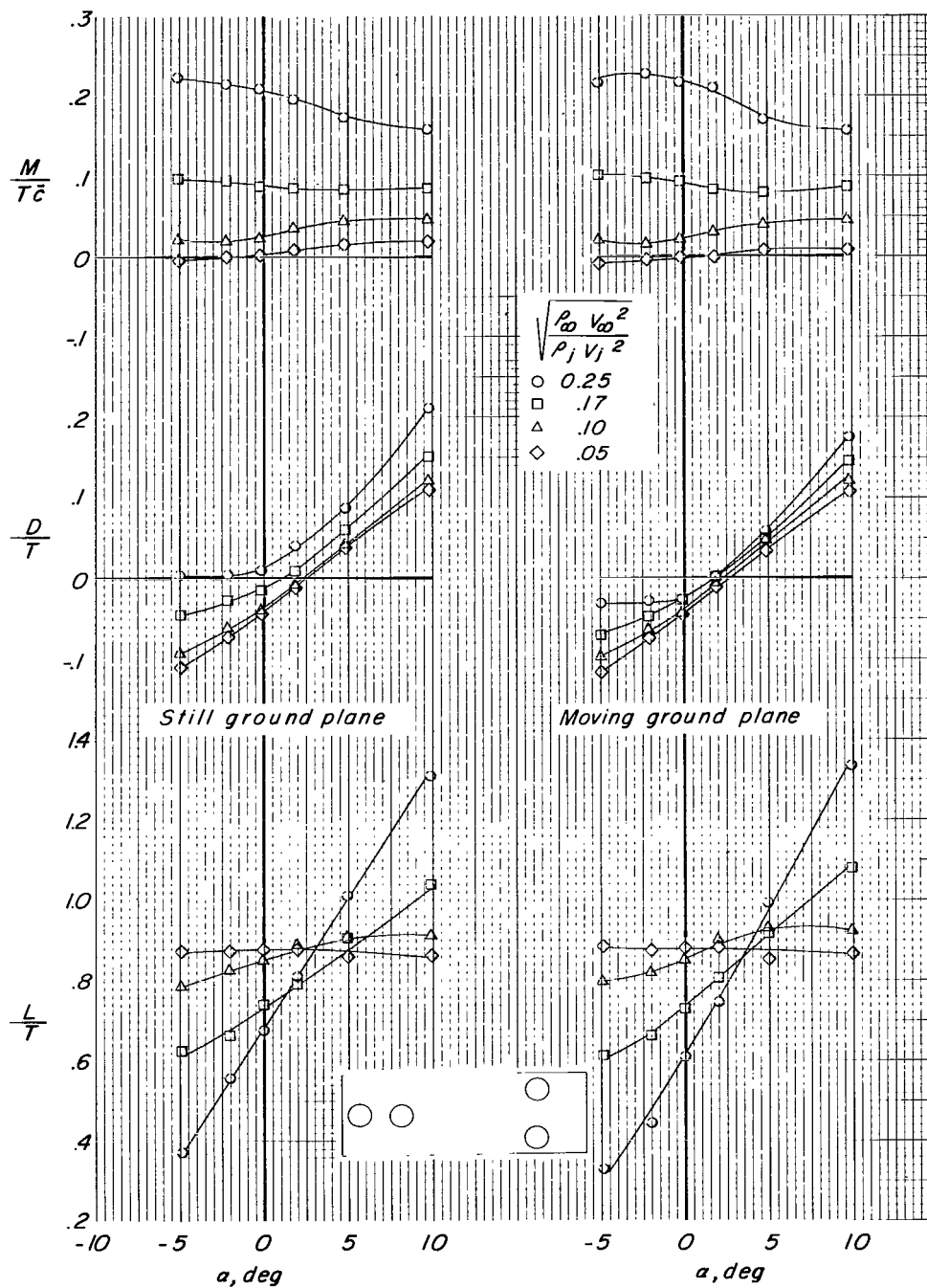
(c) Configuration 3.

Figure 9.- Continued.



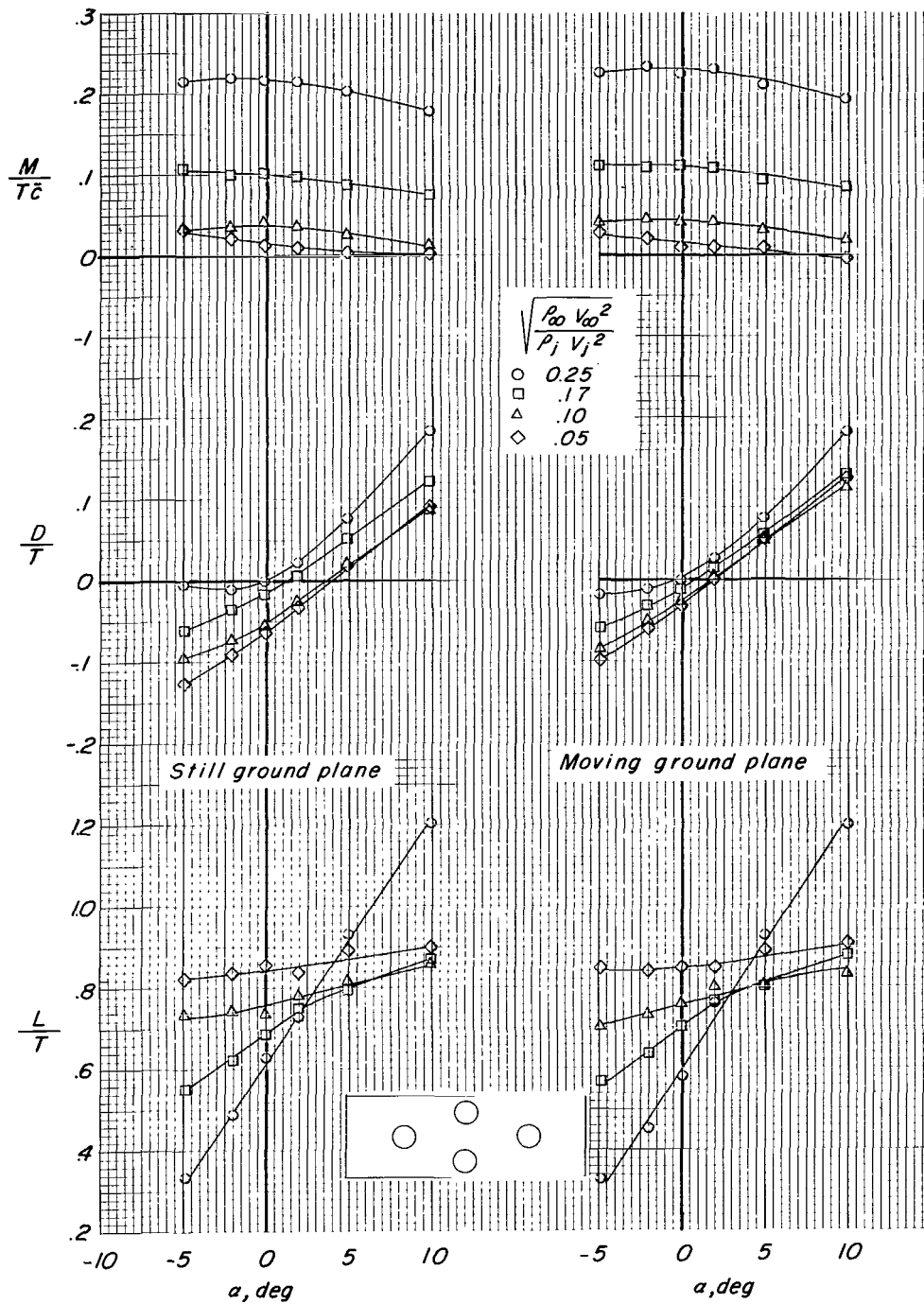
(d) Configuration 4.

Figure 9.- Continued.



(e) Configuration 5.

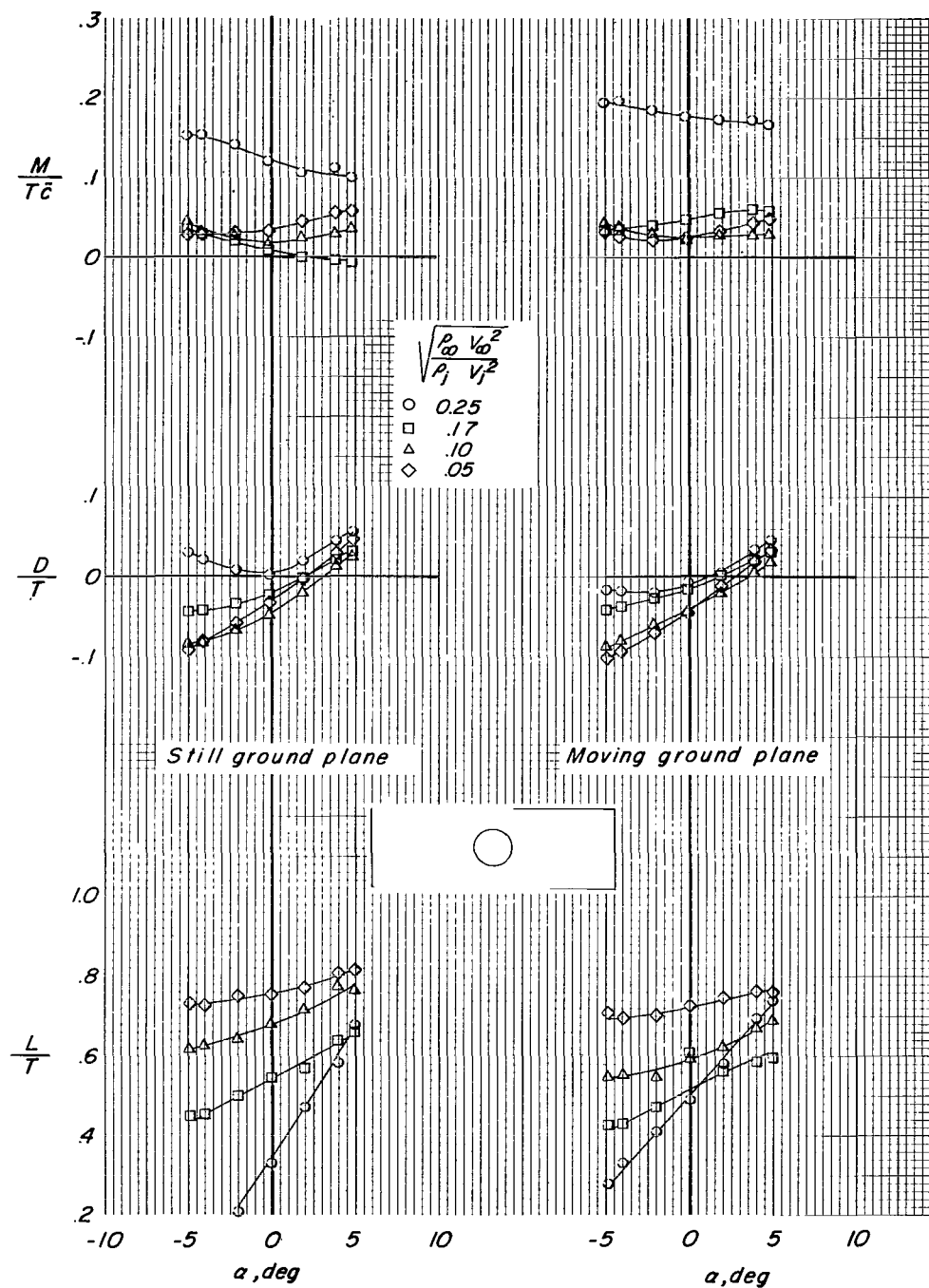
Figure 9.- Continued.



(f) Configuration 6.

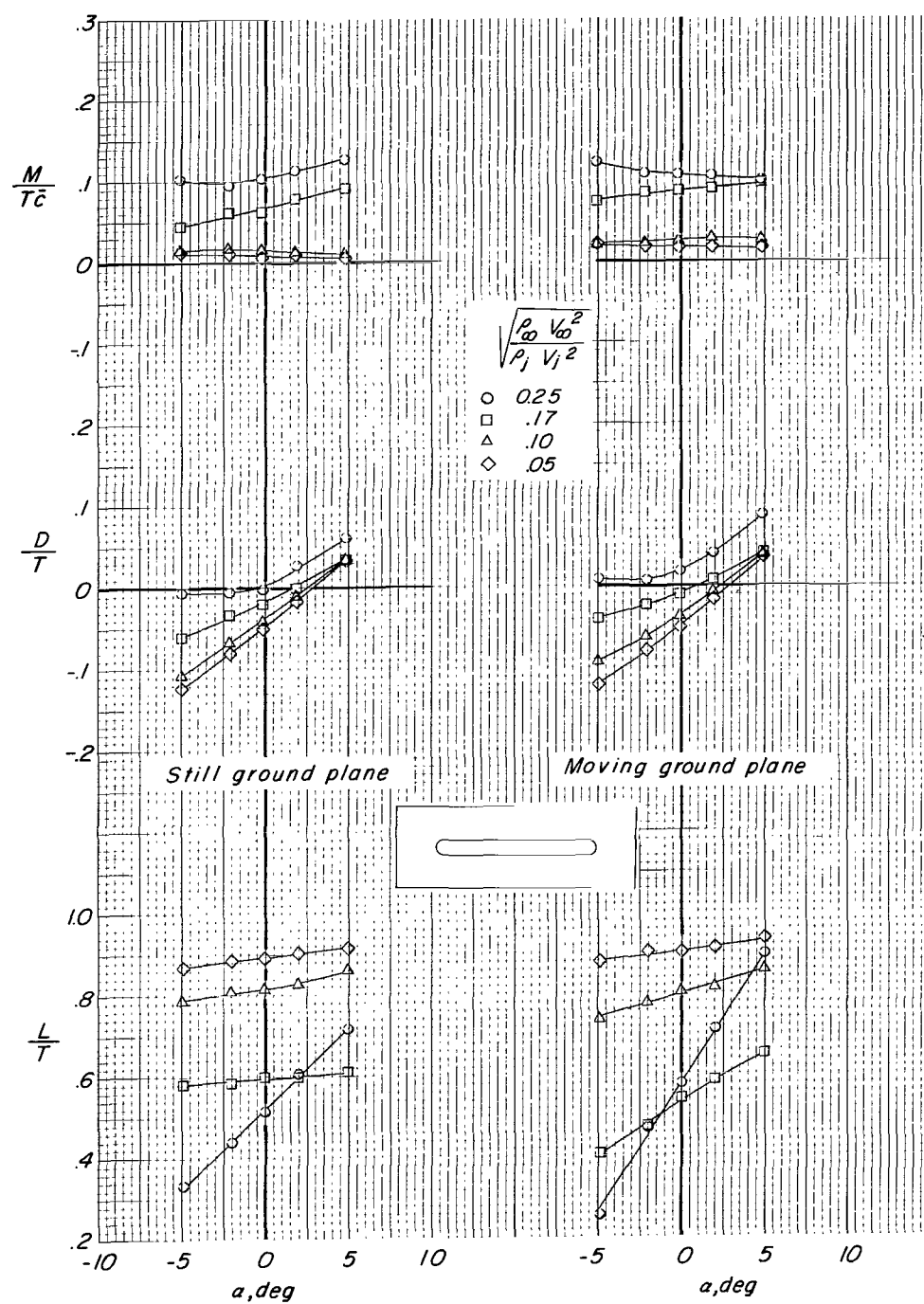
Figure 9.- Concluded.





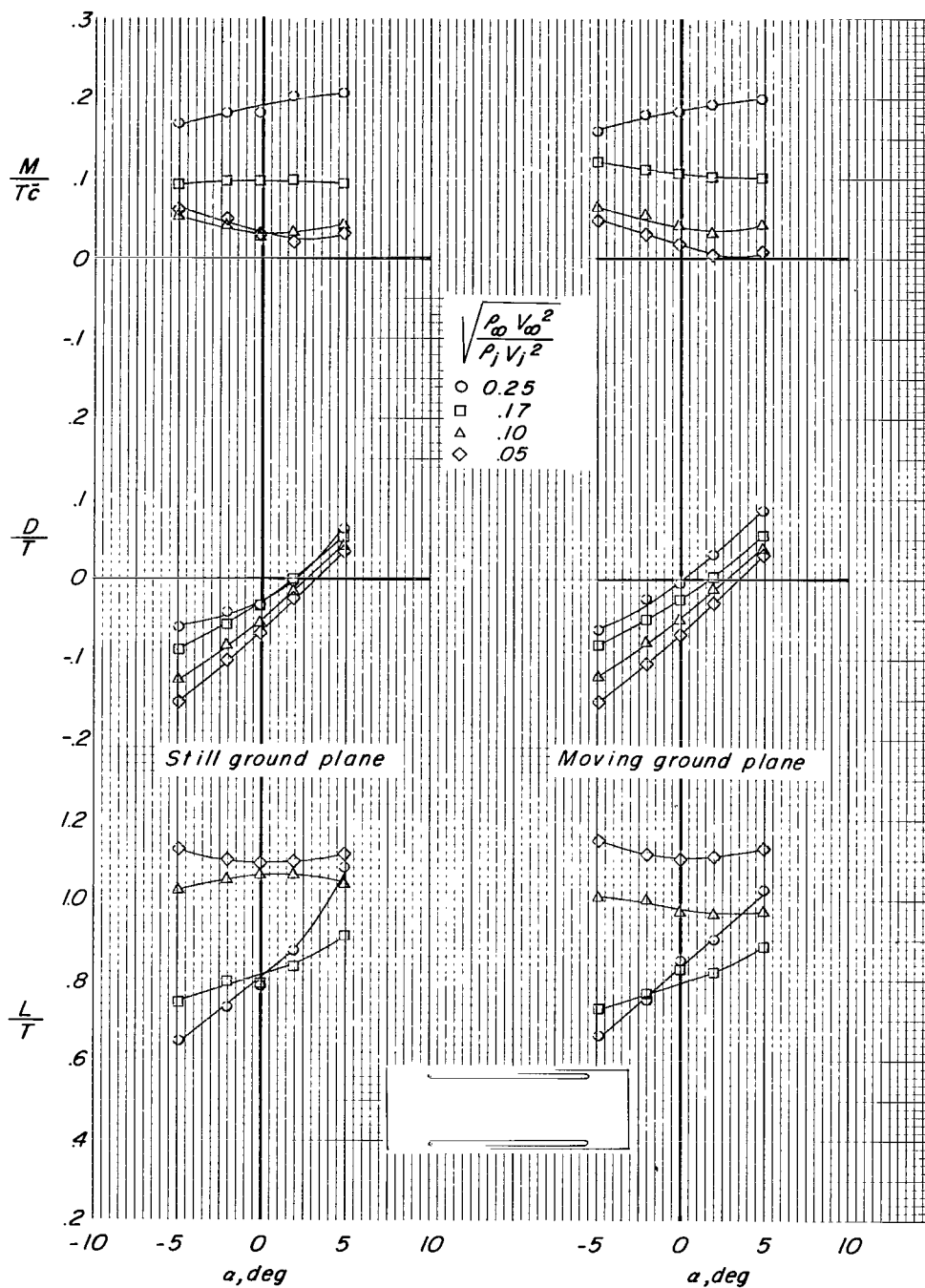
(a) Configuration 1.

Figure 10.- Longitudinal characteristics of model configurations through an angle-of-attack range at a height of 1 effective nozzle diameter from a still and a moving ground plane.



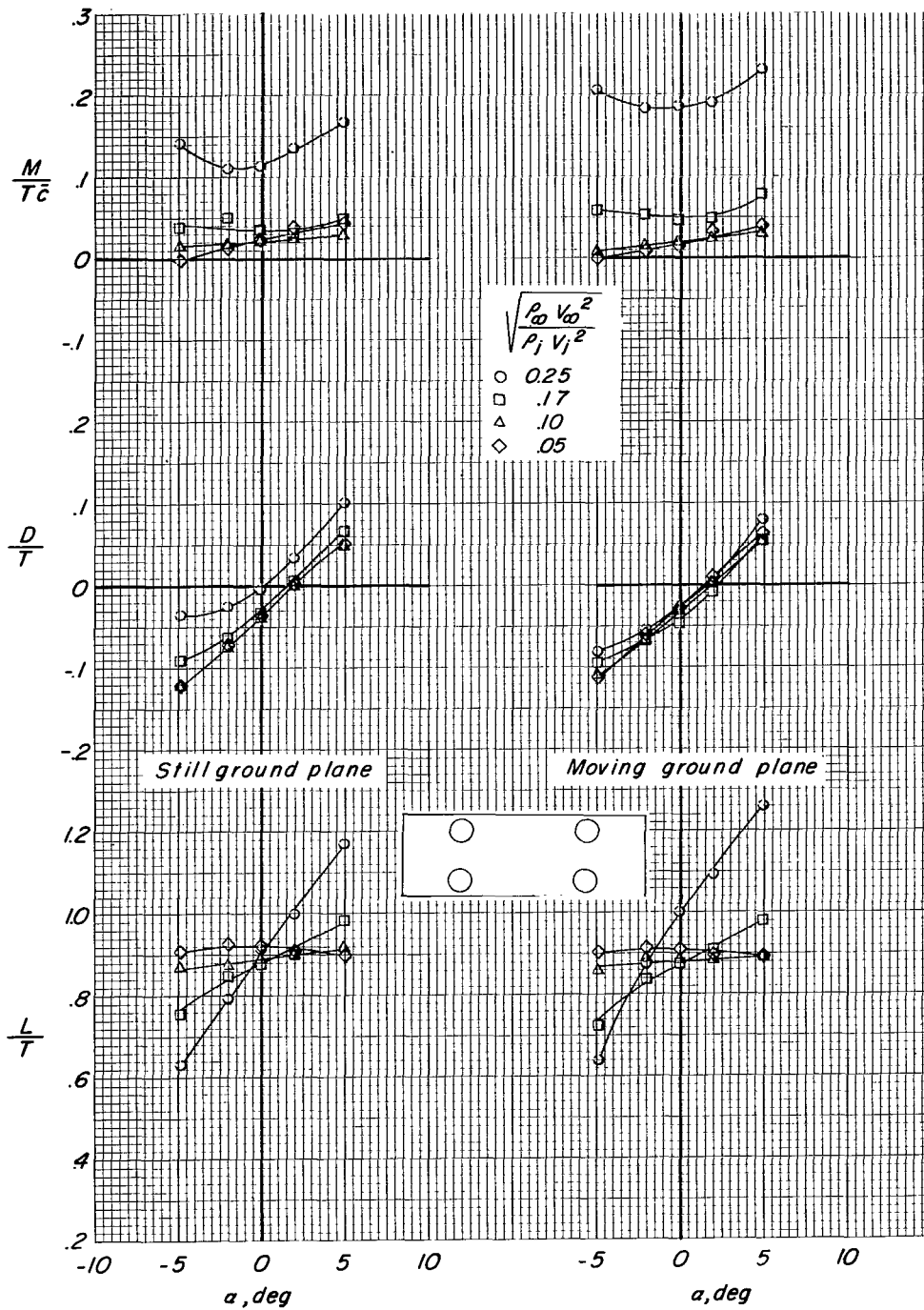
(b) Configuration 2.

Figure 10.- Continued.



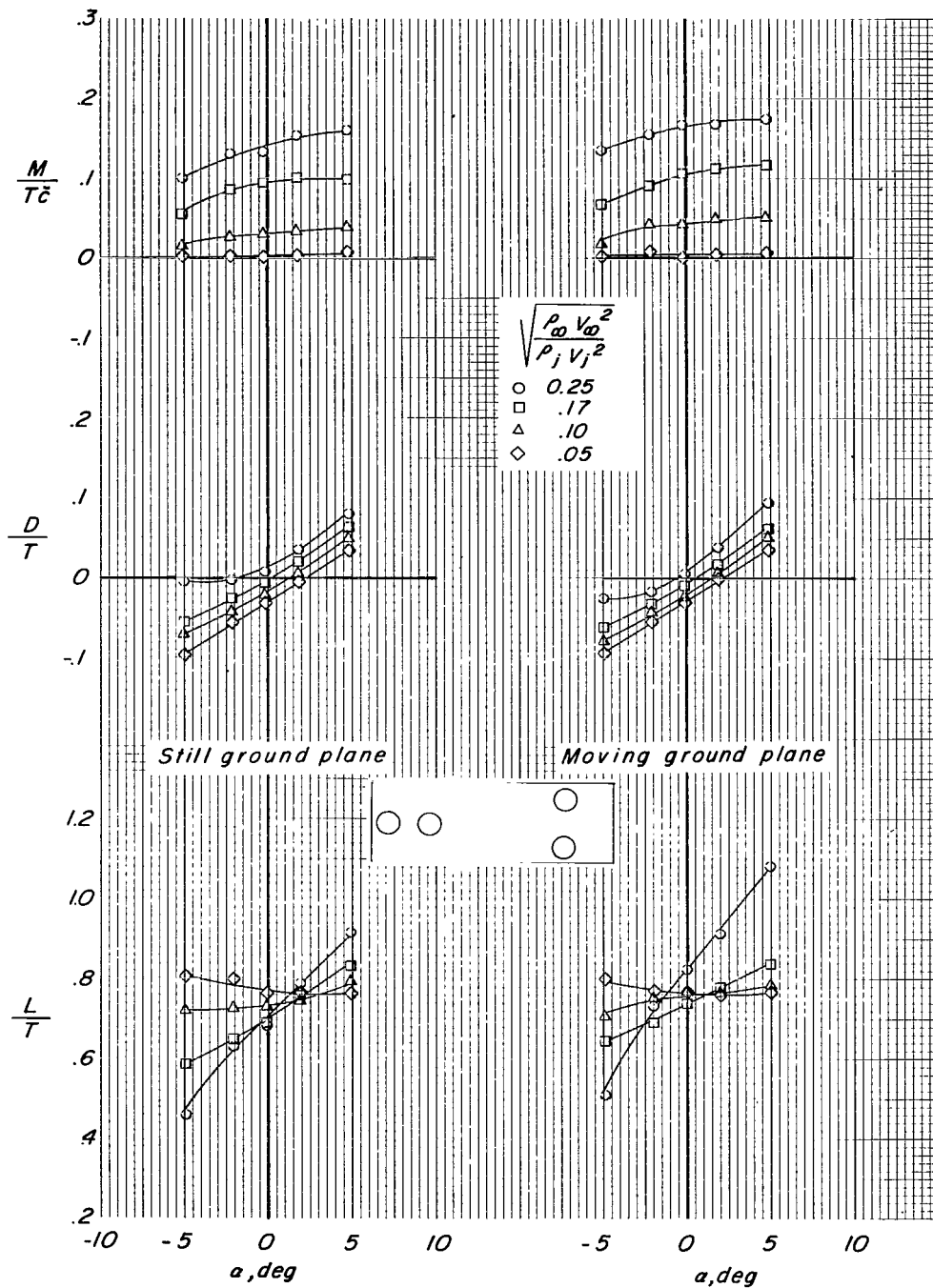
(c) Configuration 3.

Figure 10.- Continued.



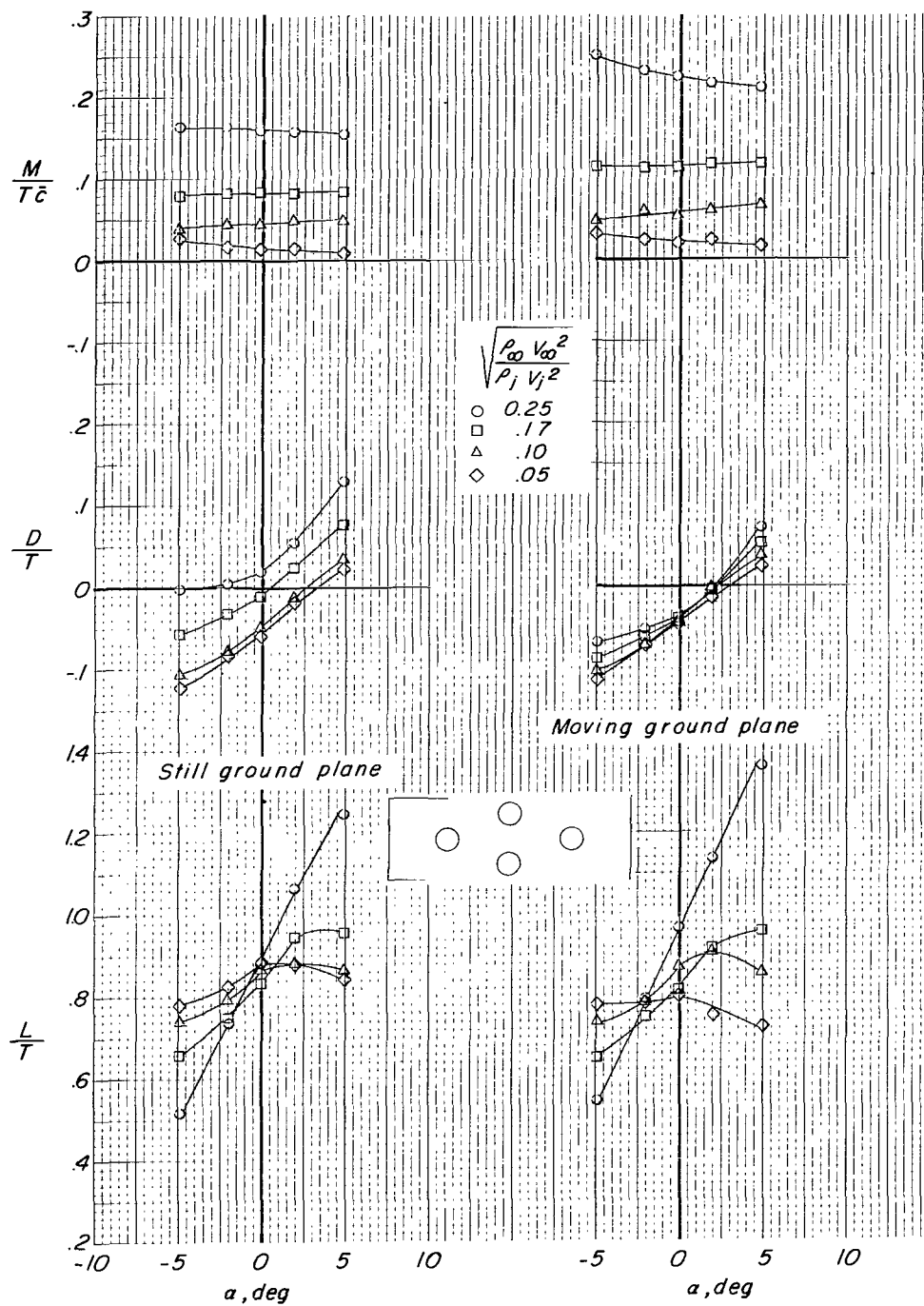
(d) Configuration 4.

Figure 10.- Continued.



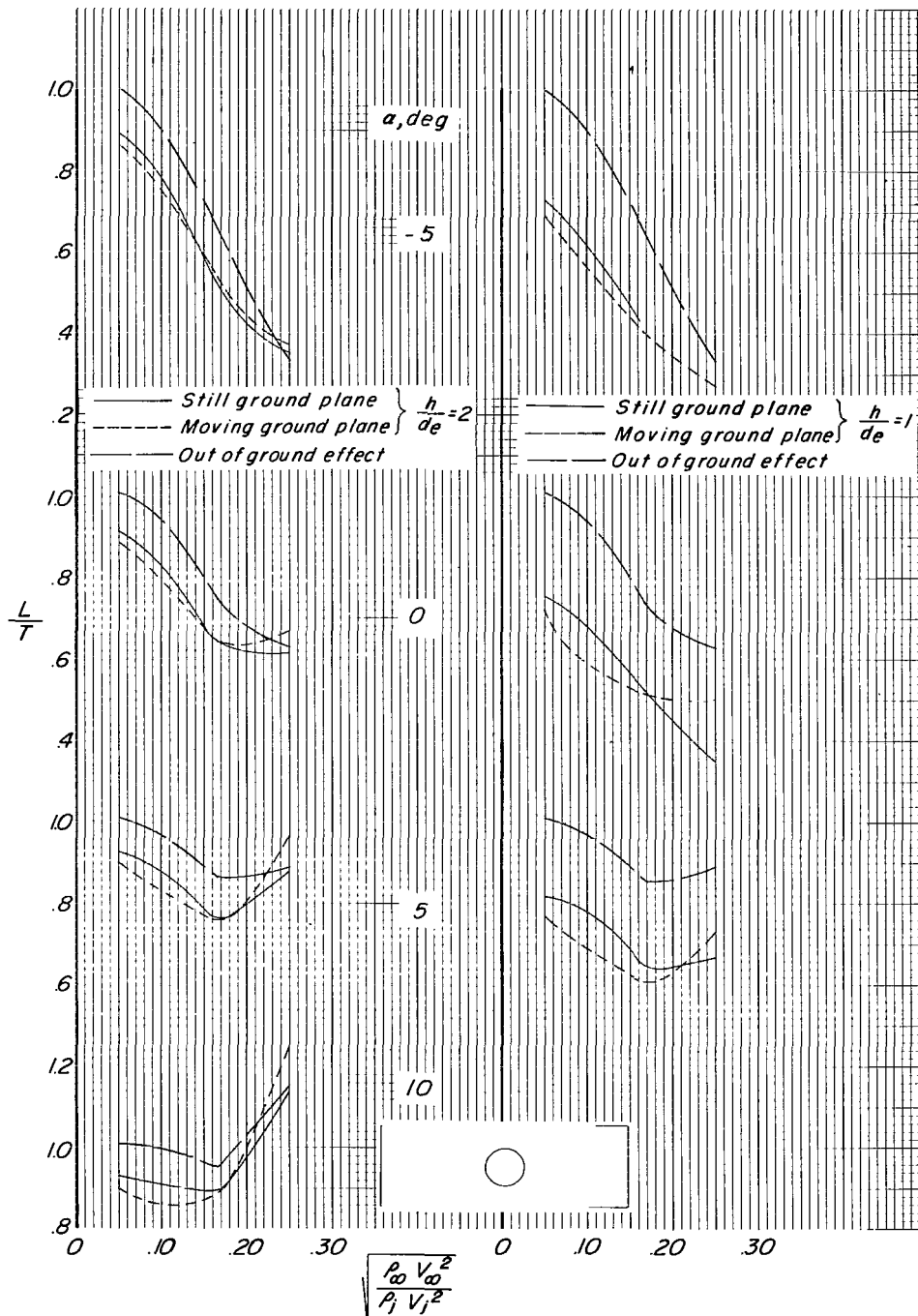
(e) Configuration 5.

Figure 10.- Continued.



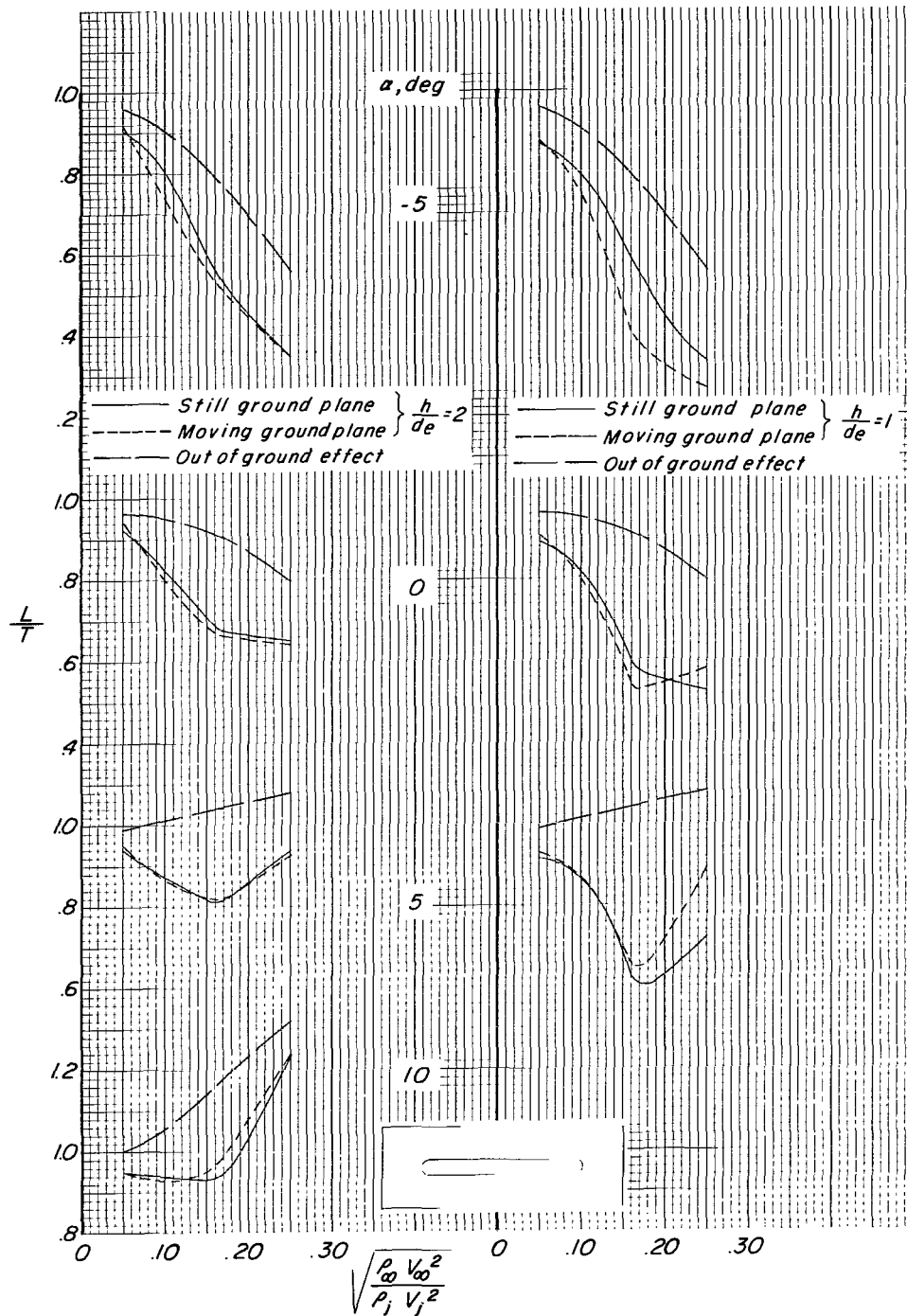
(f) Configuration 6.

Figure 10.- Concluded.



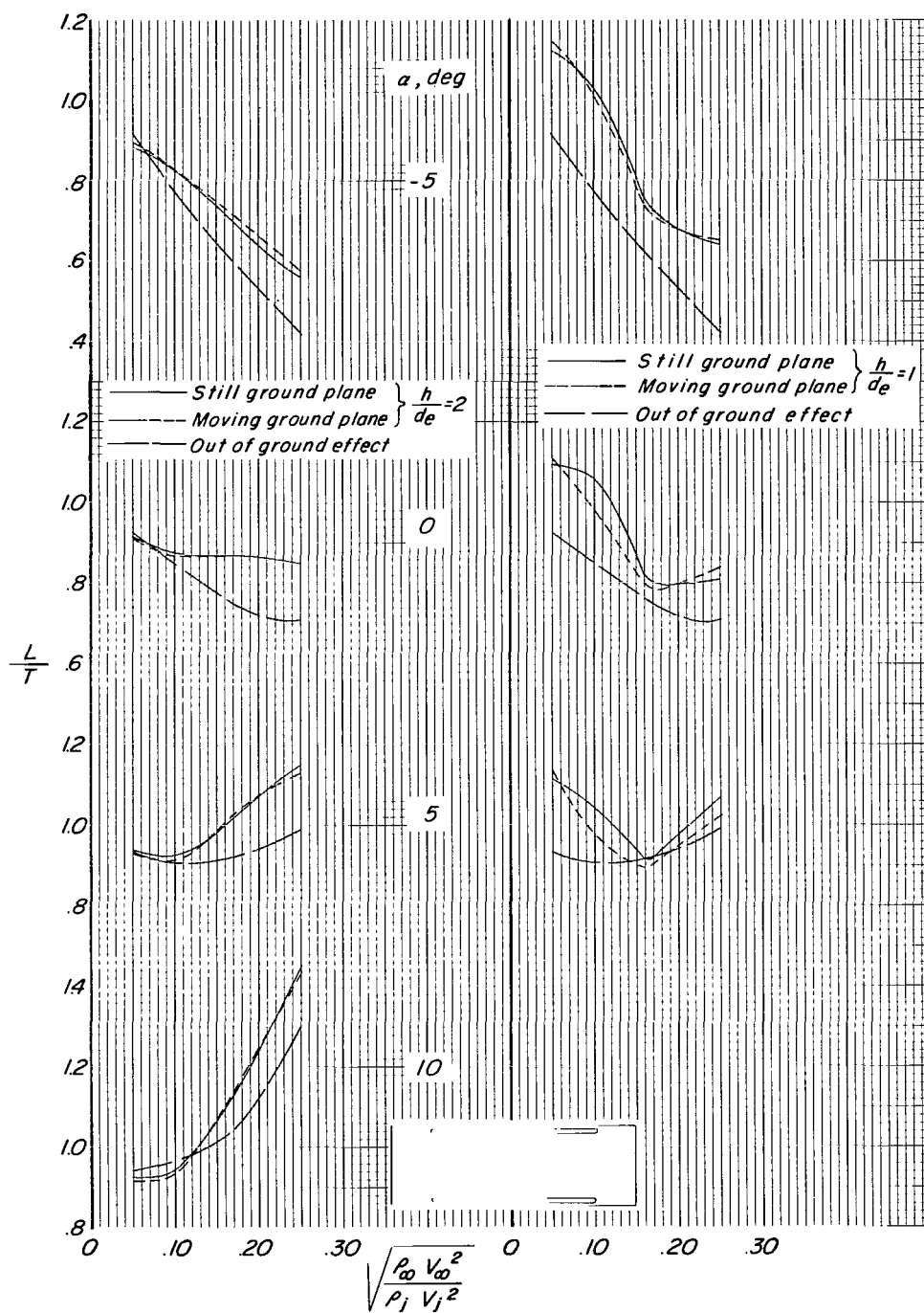
(a) Configuration 1.

Figure 11.- Comparison of effects of a still and a moving ground plane on lift characteristics of model configurations at various angles of attack through a range of effective velocity ratios.



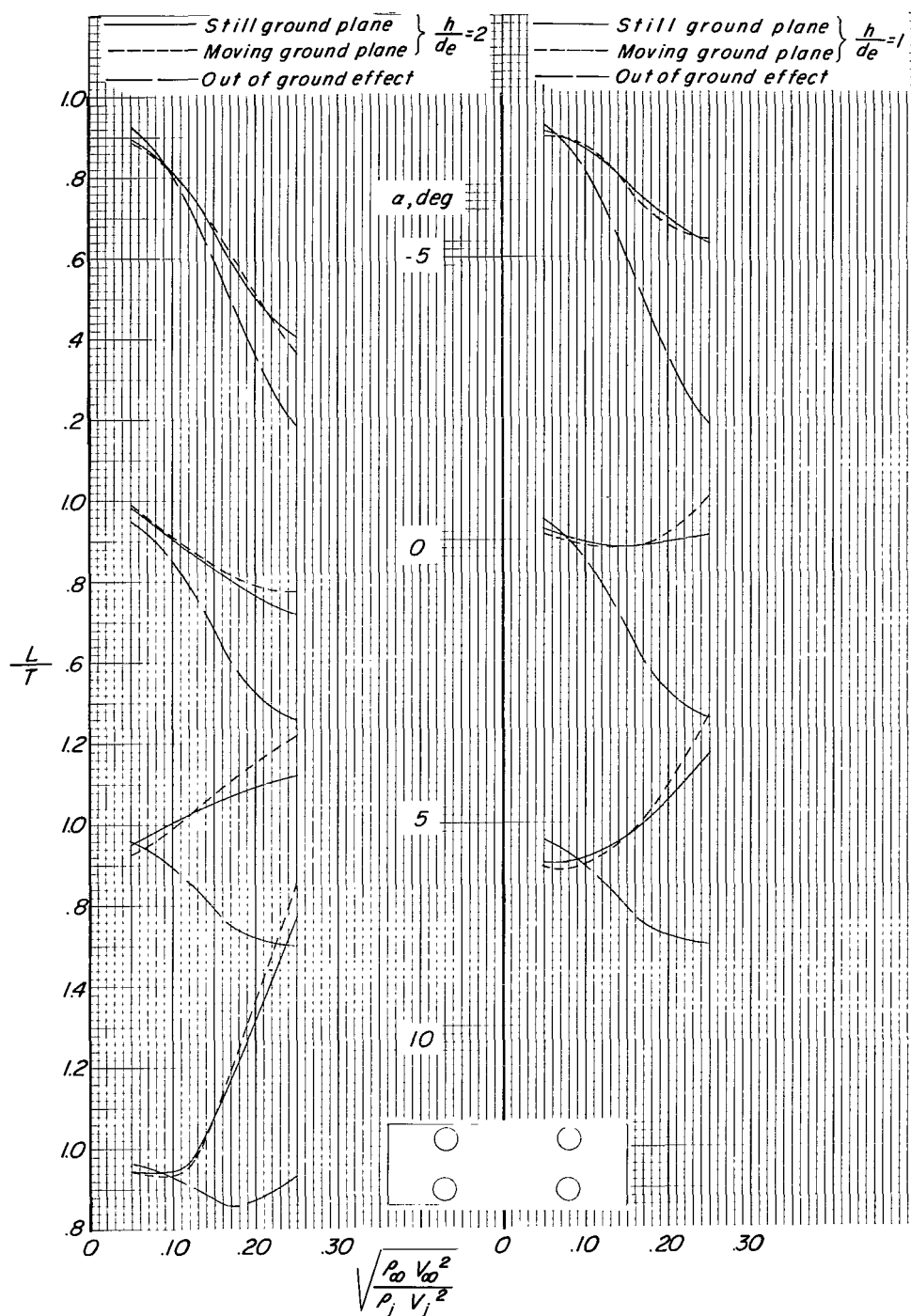
(b) Configuration 2.

Figure 11.- Continued.



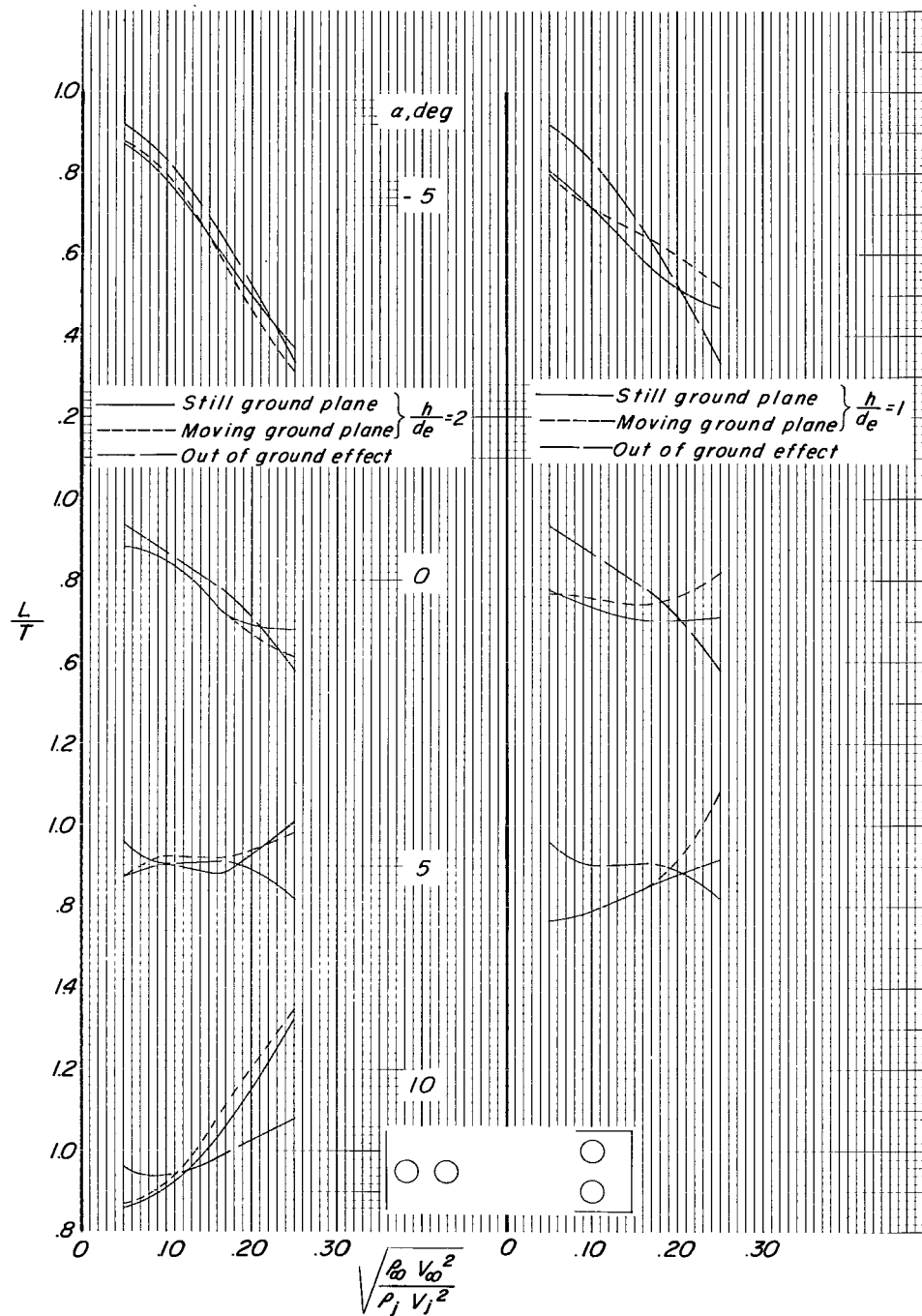
(c) Configuration 3.

Figure 11.- Continued.



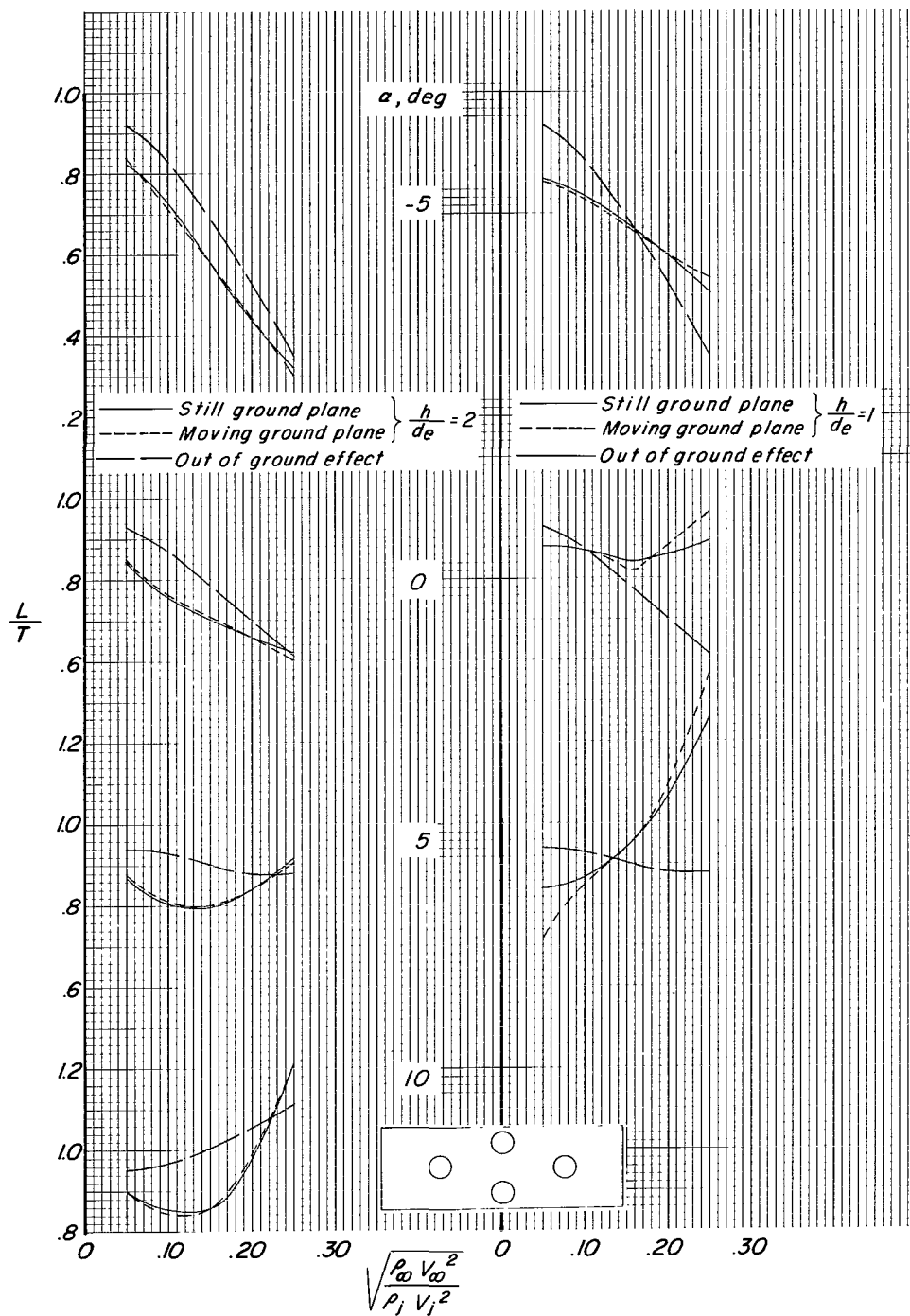
(d) Configuration 4.

Figure 11.- Continued.



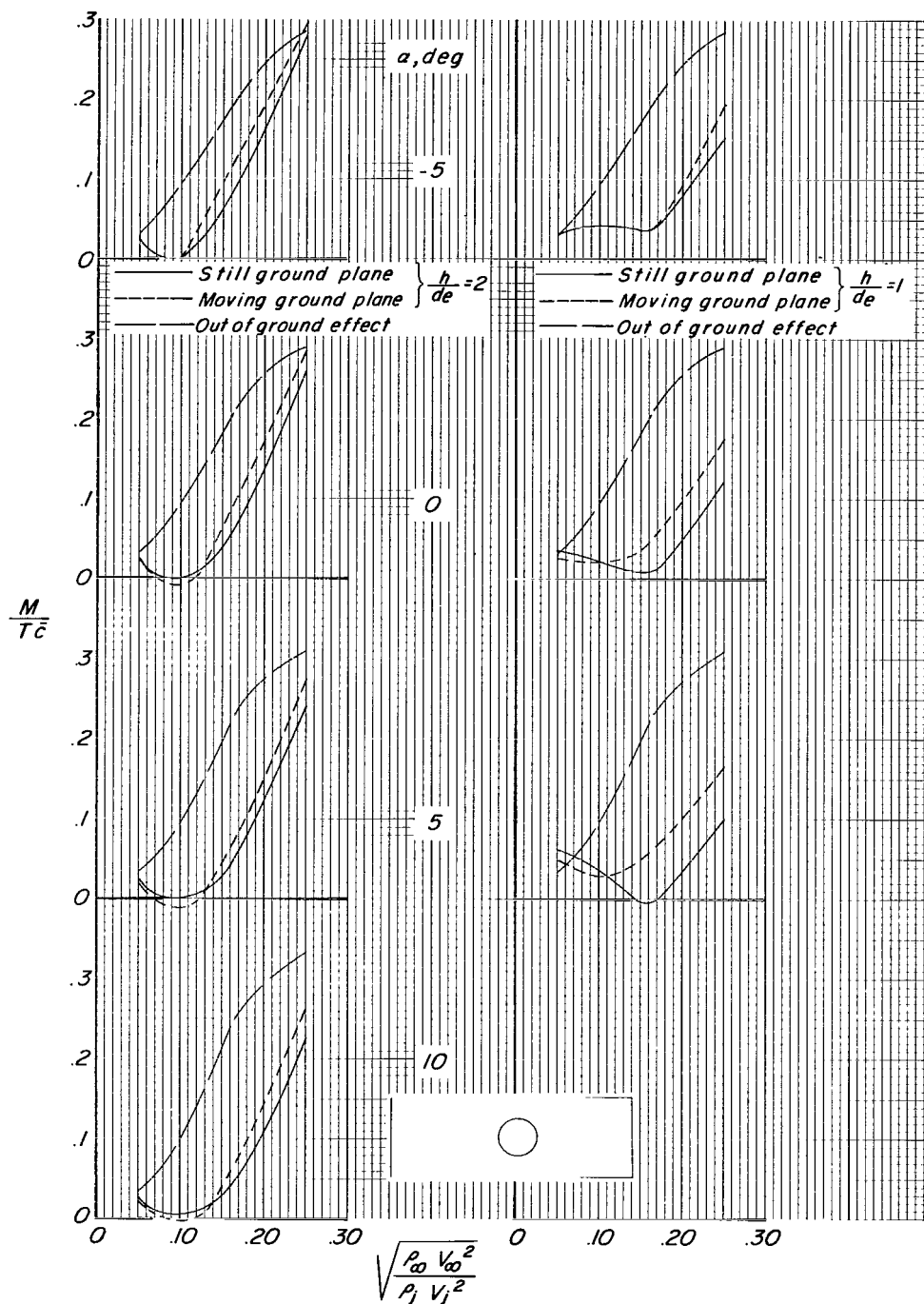
(e) Configuration 5.

Figure 11.- Continued.



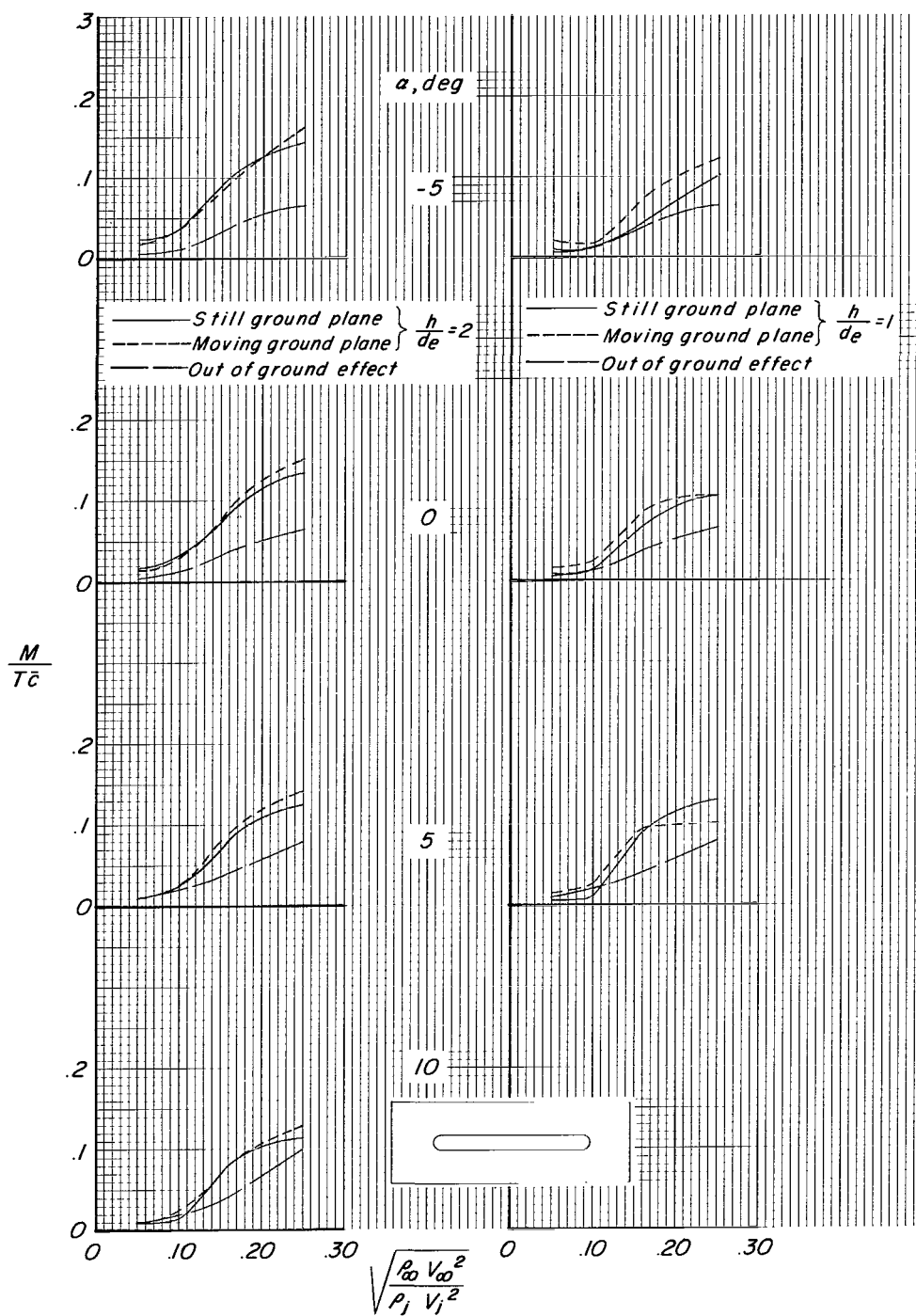
(f) Configuration 6.

Figure 11.- Concluded.



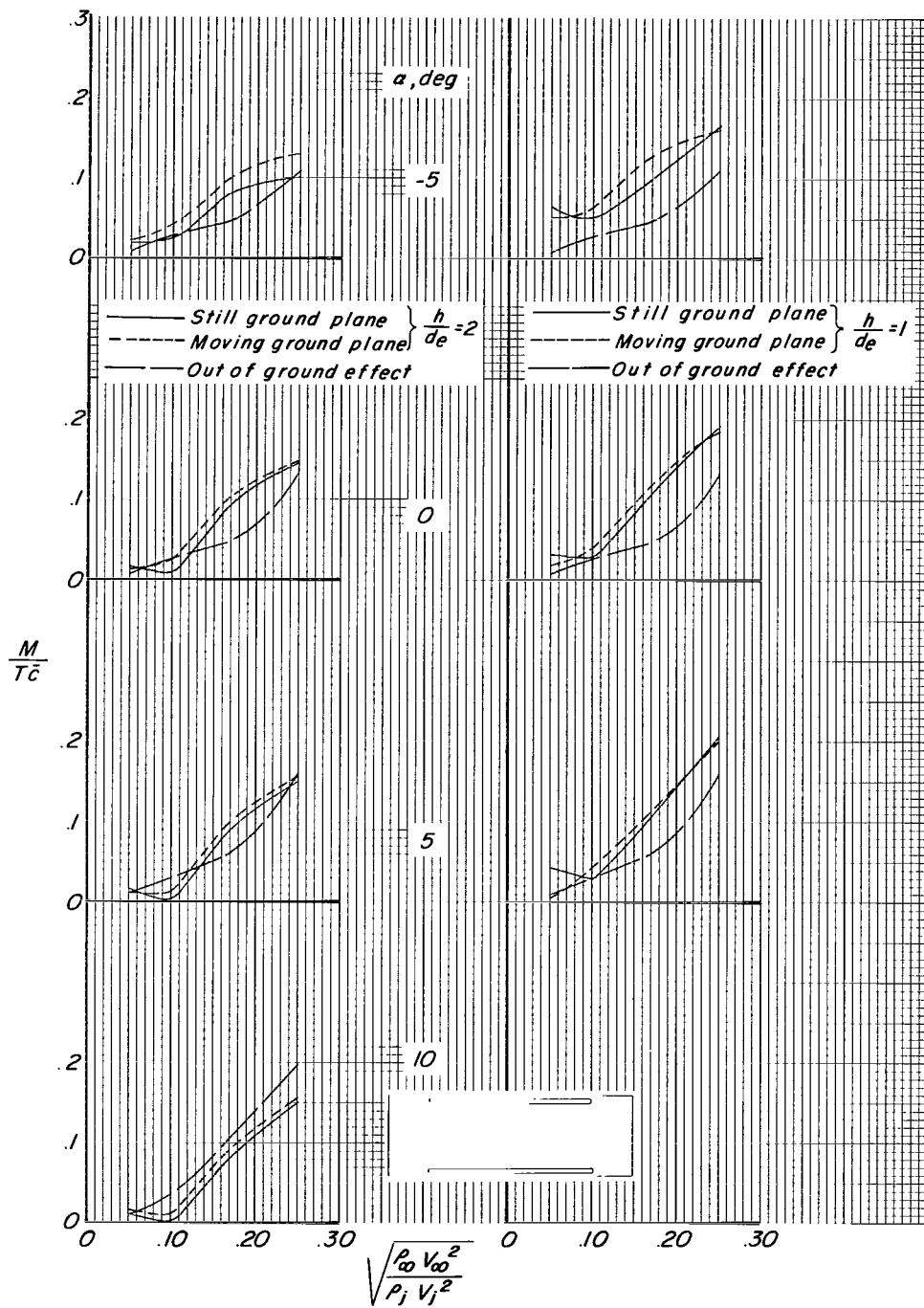
(a) Configuration 1.

Figure 12.- Comparison of effects of a still and a moving ground plane on pitching-moment characteristics of model configurations at various angles of attack through a range of effective velocity ratios.



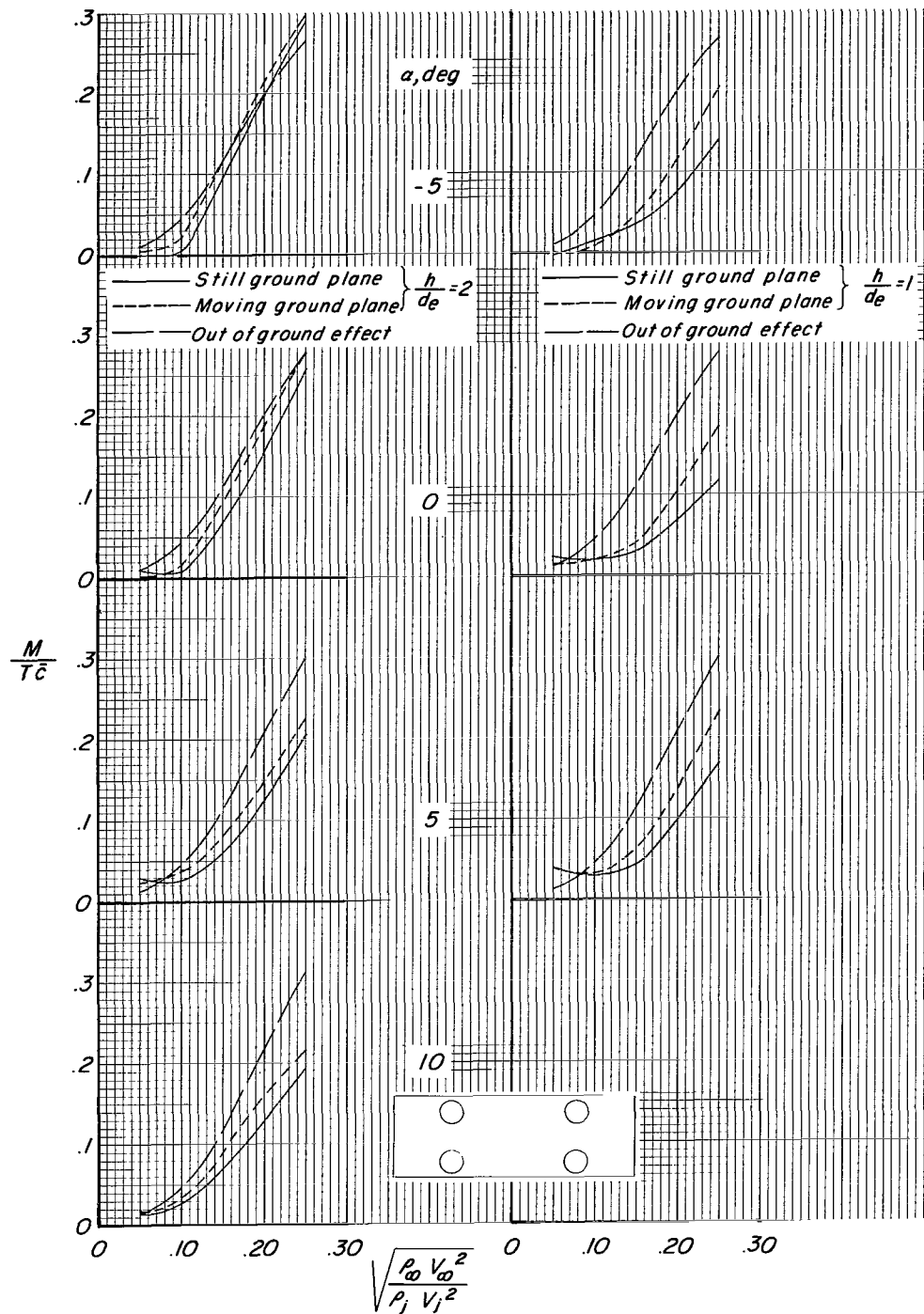
(b) Configuration 2.

Figure 12.- Continued.



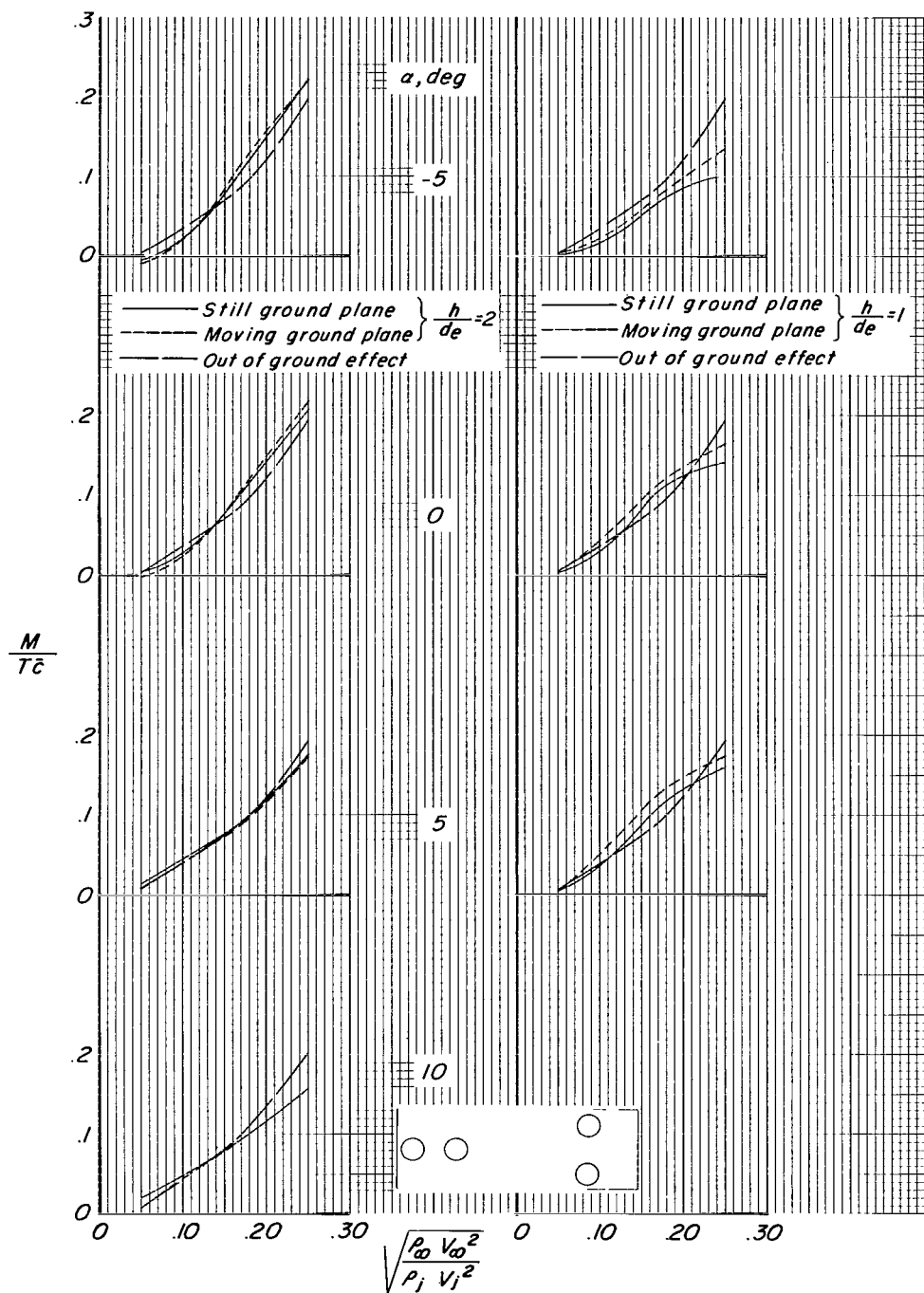
(c) Configuration 3.

Figure 12.- Continued.



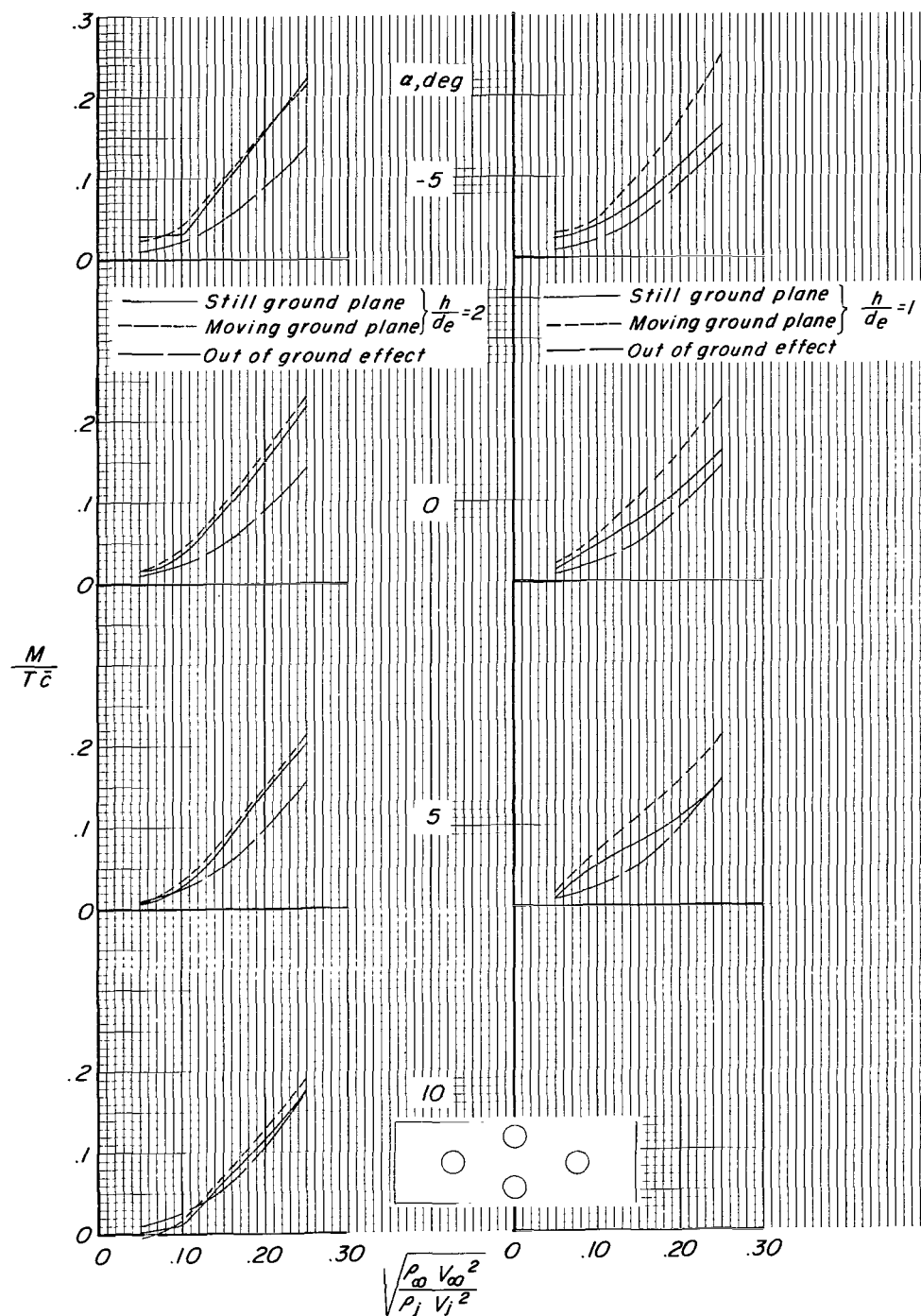
(d) Configuration 4.

Figure 12.- Continued.



(e) Configuration 5.

Figure 12.- Continued.



(f) Configuration 6.

Figure 12.- Concluded.

"The aeronautical and space activities of the United States shall be conducted so as to contribute . . . to the expansion of human knowledge of phenomena in the atmosphere and space. The Administration shall provide for the widest practicable and appropriate dissemination of information concerning its activities and the results thereof."

—NATIONAL AERONAUTICS AND SPACE ACT OF 1958

NASA SCIENTIFIC AND TECHNICAL PUBLICATIONS

TECHNICAL REPORTS: Scientific and technical information considered important, complete, and a lasting contribution to existing knowledge.

TECHNICAL NOTES: Information less broad in scope but nevertheless of importance as a contribution to existing knowledge.

TECHNICAL MEMORANDUMS: Information receiving limited distribution because of preliminary data, security classification, or other reasons.

CONTRACTOR REPORTS: Technical information generated in connection with a NASA contract or grant and released under NASA auspices.

TECHNICAL TRANSLATIONS: Information published in a foreign language considered to merit NASA distribution in English.

TECHNICAL REPRINTS: Information derived from NASA activities and initially published in the form of journal articles.

SPECIAL PUBLICATIONS: Information derived from or of value to NASA activities but not necessarily reporting the results of individual NASA-programmed scientific efforts. Publications include conference proceedings, monographs, data compilations, handbooks, sourcebooks, and special bibliographies.

Details on the availability of these publications may be obtained from:

SCIENTIFIC AND TECHNICAL INFORMATION DIVISION
NATIONAL AERONAUTICS AND SPACE ADMINISTRATION
Washington, D.C. 20546